



UNIVERSITAT  
POLITÈCNICA  
DE VALÈNCIA



ESCUELA TÉCNICA  
SUPERIOR INGENIEROS  
INDUSTRIALES VALENCIA

**Academic year:**



# GLOBAL INDEX

I.	TECHNICAL REPORT.....	3
II.	LAYOUTS .....	65
III.	BUDGET .....	73
IV.	STATEMENT OF SPECIFICATIONS.....	81





# TECHNICAL REPORT

Author: Francisco Javier Saiz Vivó

Tutor: Francisco Javier Saiz Rodriguez





## INDEX

1. Abstract .....	7
1.1. Abstract .....	7
1.2. Resúmen.....	8
1.3. Resüm.....	9
2. INTRODUCTION .....	10
2.1. Heart physiology.....	10
2.2. Extracellular bioelectric signals .....	12
2.3. ECG .....	14
2.4. ECG in sports .....	16
3. OBJECTIVES AND JUSTIFICATIONS .....	17
3.1. Objectives .....	17
3.2. Academic Justifications .....	17
3.3. Technological Justifications .....	18
4. THEORETICAL BACKGROUND .....	18
4.1. Signal characteristics .....	18
4.2. Interference sources.....	19
4.3. Reduction artifacts techniques.....	21
4.4. Safety requirements .....	21
4.5. Electrode characteristics .....	22
5. DESIGN PROCESS .....	24
5.1. Specifications.....	24
5.2. Block diagram .....	25
5.3. Theoretical design .....	25
5.4. Instrumentation amplifier and equipment protection .....	26
5.5. Isolation stage .....	29
5.6. High Pass Filter .....	30
5.7. Amplifier.....	31
5.8. Low Pass Filter .....	32
5.9. Notch Filter.....	33
5.10. Common Mode Shield Driver .....	36
5.11. Driven Right Leg.....	37
5.12. Isolated Power Supply .....	38
6. CIRCUIT DEVELOPMENT .....	39
6.1. OrCAD Capture and Layout.....	39
6.2. Manufacturing Process.....	43



7.	TESTS AND RESULTS .....	47
7.1.	Frequency Response.....	47
7.1.1.	Frequency response without the 50Hz Filter .....	47
7.1.2.	Frequency response with the 50Hz Filter .....	48
7.2.	Rejection of the common mode .....	49
7.3.	Noise Test.....	50
7.4.	Common Mode Shielded Driver Test.....	51
7.5.	Driven-Right-Leg circuit .....	52
7.6.	Test on Sport Activities.....	53
8.	VISUALISATION AND TREATMENT OF THE SIGNAL.....	57
8.1.	Objectives.....	57
8.2.	DAQ USB Device .....	57
8.3.	LabView Interface.....	57
8.4.	Code implemented .....	58
8.5.	Results .....	59
9.	CONCLUSION .....	61
10.	LIST OF FIGURES .....	62
11.	REFERENCES .....	64



## 1. Abstract

### 1.1. Abstract

The following project aims to design and develop an ECG acquisition system to use in sport activities. Therefore, this report begins with a brief introduction to the physiology of the heart and the formation of an ECG from a biological and electrical point of view. Additionally, a short analysis of the typical ECG signal is made enabling us to define the characteristics of the system. Overall, this project has been divided into four main parts.

Theoretical design.

Once defined specifications we proceed to choose the components needed to carry them out. Thus, a schematic design and a first list of components is obtained. In order to process the components and tracks distribution, it is necessary to introduce the schematic to a computer program where the design stage will end. The program is a OrCAD chosen because it is a program widely used in the workplace.

Manufacture of the plate.

When we have obtained the transparencies, we will proceed to the manufacture of the plate which can be divided into four stages: insolation, , machining (drilling) and soldering. These steps were made entirely in the lab as all the components needed were there.

Tests.

To ensure the proper functioning of the board a series of experiments were designed test wether the plate met some safety requierements and then, we conducted human experiments where the subject was connected to the plate and measures where taken while he was resting and running at 6km/h and 8km/h.

Digitization

Both the acquisition of the signal and filtering is carried out in analog form and to finish this project, the design of a virtual tool in LabView to display the signal and doing a final processing is made.

Keywords: ECG, heart, sport, amplifying, processing





## 1.2. Resumen

El siguiente trabajo de fin de curso pretende diseñar y desarrollar un sistema de adquisición de ECG para ser utilizado en actividades deportivas. Por ello, primero se realiza una breve introducción de la fisiología del corazón y de la formación de un ECG desde un punto de vista biológico y eléctrico. Además, se hace un pequeño análisis de la señal típica de ECG para luego poder definir las características de nuestro sistema para poder desarrollarlo. En conjunto, este proyecto se ha dividido en 4 partes fundamentales.

Diseño teórico.

Una vez definidas las especificaciones se procede a elegir los componentes necesarios para llevarlas a cabo. Así, se obtiene un diseño esquemático y una primera lista de componentes. Para la obtención de la distribución de componentes y pistas que luego utilizaremos para el revelado, es necesario pasar el esquemático a un programa informático donde se finalizará la etapa de diseño. El programa escogido es el OrCAD ya que es un programa muy utilizado en el ámbito laboral.

Fabricación de la placa.

Cuando hayamos obtenido las transparencias se procede a la fabricación de la placa que se puede dividir en cuatro etapas: insolado, revelado, mecanizado y soldado. Esta etapa se ha realizado en su totalidad en el laboratorio de electrónica ya que ahí es donde se encuentran los componentes necesarios.

Pruebas.

Para garantizar el correcto funcionamiento de la placa se diseñaron primeramente una serie de experimentos ideados para comprobar que la placa cumpliera una serie de requisitos mínimos de seguridad y luego se llevó a cabo la experimentación en humanos donde el sujeto se conectó a la placa y se tomaron medidas mientras éste estaba en reposo, corriendo a 6km/h y a 8km/h.

Digitalización

Tanto la adquisición de la señal como el filtrado de la misma se llevan a cabo de forma analógica y para acabar este proyecto se decide diseñar una herramienta virtual, utilizando el programa informático LabView para poder visualizar la señal y realizar un procesamiento digital posterior.

Palabras clave: ECG, corazón, deporte, amplificación, procesamiento



### 1.3. Resum

El següent treball de fi de curs pretén dissenyar i desenvolupar un sistema d'adquisició d'ECG per ser utilitzat en activitats esportives. Per això, primer es realitza una breu introducció de la fisiologia del cor i de la formació d'un ECG des d'un punt de vista biològic a més de elèctric. A més, es fa un xicotet anàlisi del senyal típic d'ECG per poder després definir les característiques del nostre sistema per després poder desenvolupar-lo. En conjunt, aquest projecte s'ha dividit en 4 parts fonamentals.

Disseny teòric.

Una vegada definides les especificacions es procedeix a triar els components necessaris per dur-les a terme el millor possible. Així, s'obté un disseny esquemàtic i una primera llista de components. Per a l'obtenció de les transparències que després utilitzarem per al revelat, cal passar el esquemàtic a un programa informàtic on es finalitzarà l'etapa de disseny. El programa triat és el OrCAD ja que és un programa molt utilitzat en l'àmbit laboral.

Fabricació de la placa.

Quan haguem obtingut les transparències es procedeix a la fabricació de la placa que es pot dividir en quatre etapes: insolat, revelat, mecanitzat i soldat. Aquesta etapa s'ha realitzat en la seua totalitat en el laboratori d'electrònica ja que aquí és on es troben els components necessaris.

Proves.

Per garantir el correcte funcionament de la placa es van dissenyar primerament una sèrie d'experiments ideats per comprovar que la placa complia una sèrie de requisits mínims de seguretat i després es va dur a terme l'experimentació en humans on el subjecte es va connectar a la placa i es van prendre mesures mentre aquest estava en repòs, corrent a 6 km/h 8km/h.

Digitalització.

Tant l'adquisició del senyal com el filtrat del mateix es duen a terme de forma analògica i per acabar aquest projecte es decideix dissenyar una eina virtual en el programa informàtic LabView per poder visualitzar el senyal i fins i tot seguir filtrant.

Paraules clau: ECG, cor, esport, amplificació, procesament

## 2. INTRODUCTION

In order to fully understand the objective of this project, a brief introduction explaining the generation of the electrocardiogram, hereinafter referred to as ECG, is needed. This introduction will cover a description of the physiology of the heart and how its biological cycle depends on the generation of potential signals that result in the ECG and the importance of ECG in sports, which is the main focus of this project.

### 2.1. Heart physiology

The ECG is basically a non-invasive way of measuring the electrical activity of the heart by registering the extracellular potentials generated by it. Within the heart, two different types of fibres are capable of generating electrical activity: muscular fibres responsible for the heart's contraction and special fibres which are used to propagate the potentials throughout the myocardium. In order to fully describe this process, we need to briefly explain the heart's anatomy and the electric potentials involved in a full cardiac cycle. The heart is comprised by 4 chambers: two atria and two ventricles which are connected by the atrioventricular valves also known as the tricuspid or right valve and the mitral or left valve. The ventricles are separated from the aorta and the pulmonary artery by the semilunar valves also known as the aortic and the pulmonary and both ventricles are separated by the interventricular septum. The interior walls of the ventricles are called the endocardium, the middle part the myocardium and the exterior of the heart the epicardium. The heart is also surrounded by a double-membrane sack called the pericardium. Figure 2-1 shows a diagram of the heart.

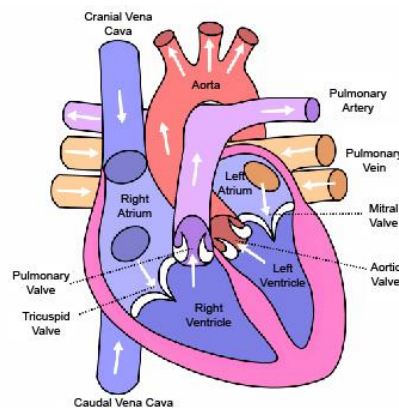


Figure 2-1 – Heart's physiology [1]

The heart acts as a pump which in order to continuously provide a stream of blood, contracts itself rhythmically giving forth the cardiac cycle. To do so effectively, the muscles in the myocardium has a swirling pattern as seen in Figure 2-2.

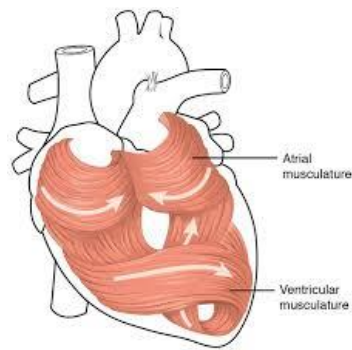


Figure 2-2 – Myocardium muscles [2]

The heart has specialized cells in the sinoatrial node responsible for generating autonomously the electrical impulses used to contract these muscles. This property is called autorhythmicity. As mentioned before, a second system of specialized fibres is in charge of distributing this electric impulse throughout the cardiac muscle.

The heart cycle can be described in many ways, two of which are the biological and the electrical. To understand the relationship between the physical response to the electrical impulse and to the ECG, both approaches must be described. Biologically speaking, the heart cycle has two main stages (the ventricular diastole and systole) that can then be divided into sub-stages which are summarized in the following image.

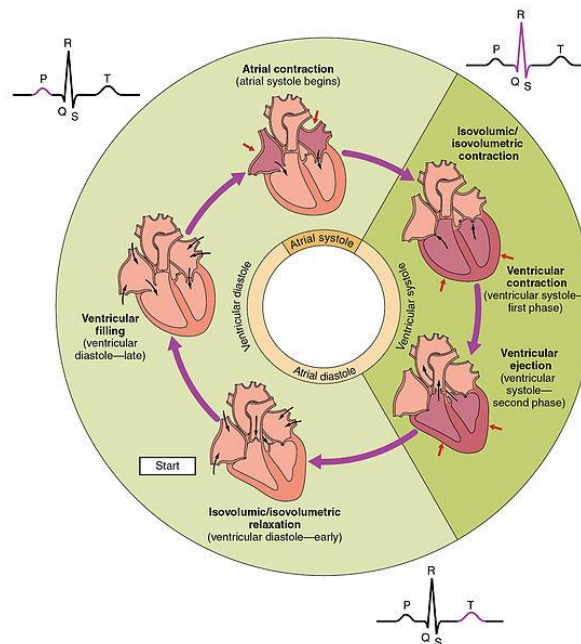


Figure 2-3 – Complete heart cycle [3]

Firstly, in the ventricular filling or late diastole, the atrioventricular valves open and the ventricles get filled with blood. When the ventricle is almost full, there is a small flow of blood directly from the veins. This process is called diastasis. The last phase of the diastole is the atrial systole, during which the atria contract so that the remaining blood inside them flows into the ventricles. This phase is responsible for filling almost one third of the ventricles. The second

stage or the systole starts with the isometric ventricular contraction, which results in an increase of pressure until the ventricular ejection takes place. This phase takes 3 times longer than the contraction. Even as the pressure decreases, blood keeps flowing due to ventricular contraction in a process called protodiastole. Finally, the isovolumetric relaxation takes place where all the ventricular fibres relax and the cycle starts again.

## 2.2. Extracellular bioelectric signals

The potential signals are responsible for the physical activity of the heart and need to be studied to fully describe the ECG generation.

Some specialized cells that can be found in the body such as neurones and muscular cells have excitable membranes that undergo important changes in their behaviour when exposed to depolarising stimuli. This produces a cellular electrical activity called the action potential. ECG and EEG (electroencephalograms) are examples of signals that are usually measured on the body surface. For this reason, extracellular bioelectric signals started being used for medical purposes.

Extracellular signals occur due to intracellular potentials i.e. the action potential. When there is an action potential, different types of currents go through the cell membrane. There are ionic currents that physically breakthrough the cell membrane and also displacement currents that are created by the capacitive characteristic of the membrane.

These currents circulate into and out of the cells creating differences in potential that propagate throughout the body until its surface were can be detected using contact electrodes. Many have tried to find a relationship between intra and extracellular potentials and various mathematical methods have been developed however, this project will be focused on designing a system for measuring the extracellular potential and will not go into detail on the mathematical approach.

Continuing with the previously description of the biological processes involved in the cardiac cycle, and in order to study the ECG waveforms, the different stages of the action potentials of a myocardial cell should be understood. The action potential in a cell are caused by the difference in the ionic composition of the intra and extracellular regions and are dependent of the semipermeable property of the cell membrane. The diffusible ions that originate the electric activity are mainly sodium  $\text{Na}^+$ , potassium  $\text{K}^+$ , and calcium  $\text{Ca}^{2+}$ . These action potentials have 5 phases numbered 0 to 4 as shown in Figure 2-4, while Figure 2-5 shows the effect of the different ions on the action potential.

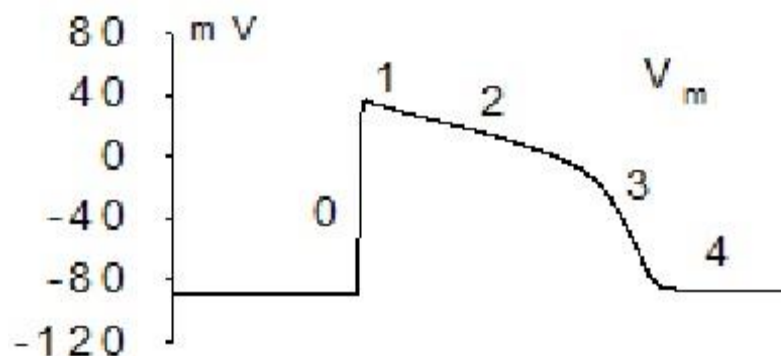


Figure 2-4 – Action potential development

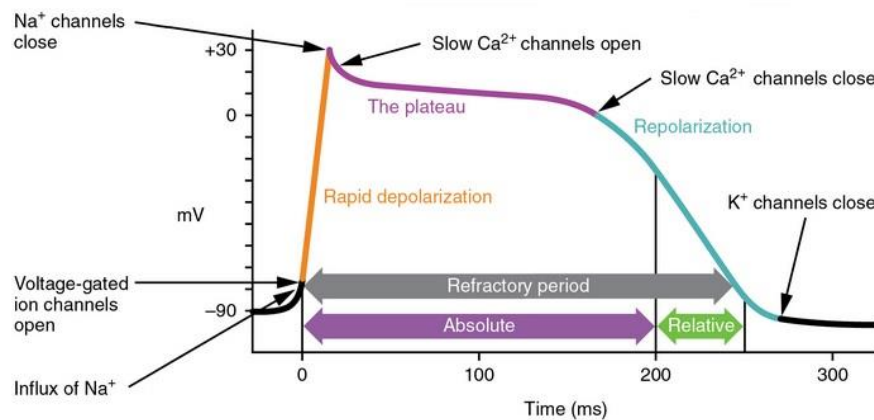


Figure 2-5 – Ionic exchange present in action potential [4]

Phase 0 corresponds to a rapid depolarization, phases 1, 2 and 3 the repolarization and phase 4 the electric diastole. The repolarization consists of 3 stages, an initial stage (phase 1) that represents a brief repolarization which results on an intracellular potential of almost zero, a second stage (phase 2) of slow repolarization also known as plateau and a final stage (phase 3) called rapid repolarization where the potential returns to its baseline. Phase 4 corresponds to the resting membrane potential when the cell is not being stimulated (-85 to -95 mV).

As these phases occur, the electrical activity which is generated spreads throughout the body and is registered on the body surface by the contact electrodes giving forth the ECG. The ECG generation depends on four electrophysiological processes: the formation of the electrical impulse developed in the sinoatrial node, the transmission of this impulse through the specialized fibres, the activation (depolarization) and the recuperation (repolarization) of the myocardium. Figure 2-6 shows the typical action potentials in the principal cardiac structures and their combined effect resulting in the ECG signal recorded on the body surface.

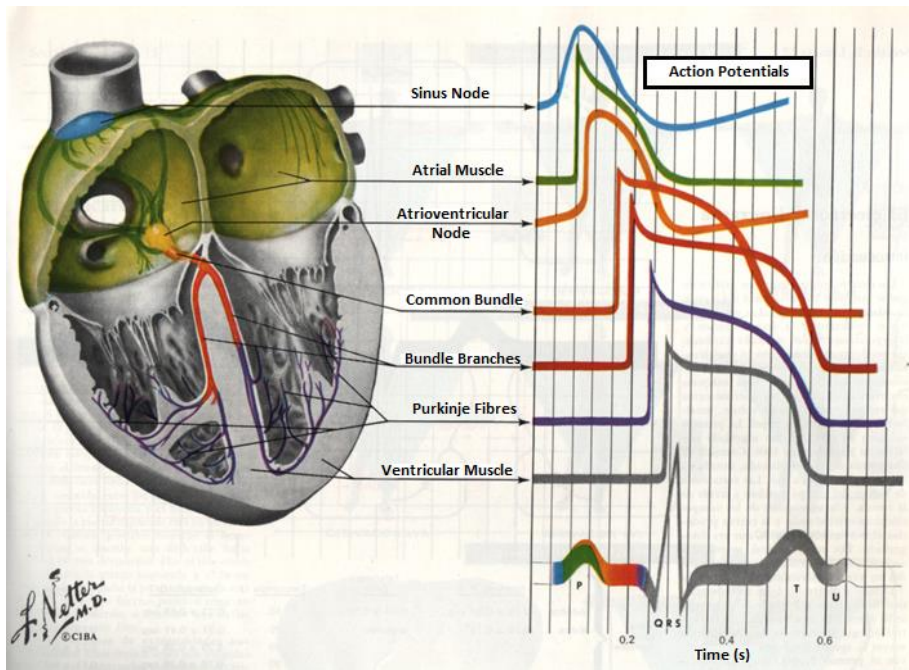


Figure 2-6 – Relationship between action potentials and the ECG [5]

### 2.3. ECG

This project will focus on the measurement of the potentials generated by the heart. Since 1903 when Willem Einthoven registered the first ECG using a galvanometer, the ECG has become an essential tool for clinic analysis and diagnosis. As can be observed in the image bellow, Einthoven's ECG system was very rudimental and used buckets filled with a solution of water and salt to improve the electrode-skin interface.

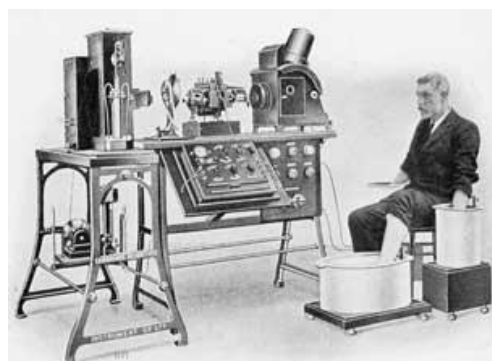
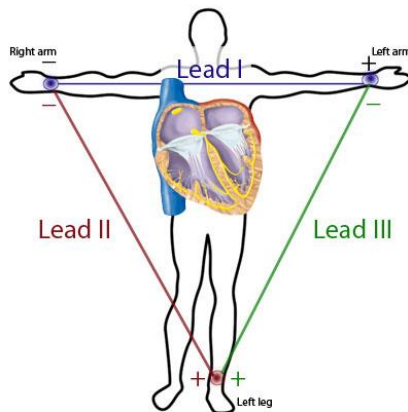


Figure 2-7 – W.Einthoven's first ECG system [6]

For the ECG to be measured, the electrodes must be placed in certain parts of the body and the signal depends on the recording location. Einthoven studied the relationship between the location and the ECG obtained and developed an equilateral triangle where the heart constituted the center. This triangle was called Einthoven's triangle, and is used when determining the electrical axis of the heart as it is shown in Figure 2-8. The potential difference

between the axis of Einthoven's triangle were called standard leads I, II and III which are summarized in Table 2-1.



<b>LEAD I</b>	RIGHT ARM (-) TO LEFT ARM (+)
<b>LEAD II</b>	RIGHT ARM (-) TO LEFT LEG (+)
<b>LEAD III</b>	LEFT ARM (-) TO LEFT LEG (+)

Table 2-1 – Standard Leads

Figure 2-8 – Standard Leads [7]

Note that there is a clear relationship between the leads:

$$L_I + L_{III} = L_{II} \quad (1)$$

Measuring the ECG in the different leads results in different ECG waveforms. These differences are shown in the following image.

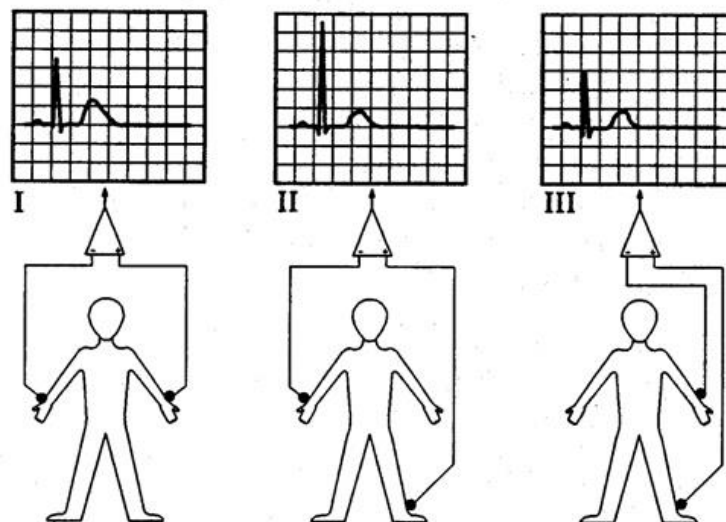
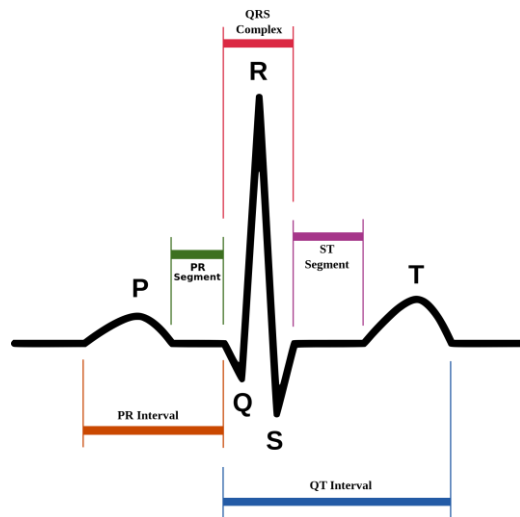


Figure 2-9 – ECG depending on the lead used [8]



The standard ECG pulse have distinct intervals that were named by Einthoven. Figure 2-10 shows a typical scalar electrocardiographic lead while Table 2-2 shows the usual durations of each of the intervals.



P-R Interval	200 ms
Q-T Interval	310 ms
P-R Segment	100 ms
S-T Segment	140 ms
Q-R-S Complex	100 ms

Table 2-2 – ECG interval duration [8]

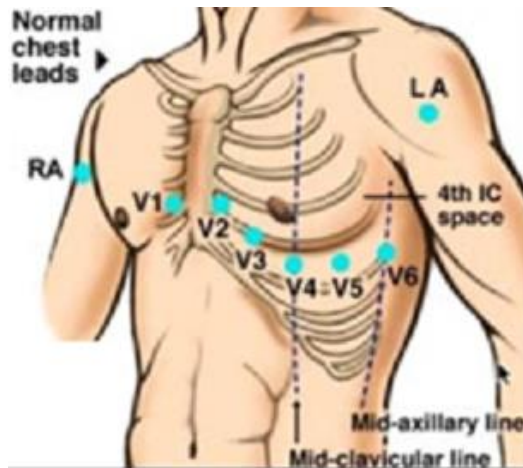
Figure 2-10 – Typical ECG waveform [9]

The first wave that usually appears in an ECG is the P wave, which is produced by the atrial depolarization during the atrial systole. Its low amplitude is due to the fact that the number of atrial fibres, responsible for the atrial contraction, is relatively smaller compared to the number of myocardial fibres responsible for the rest of the ECG waves. The next three waves constitute the QRS complex. These waves are product of the contraction of the ventricular fibres. First, the Q wave which has a very low amplitude and has a negative polarity, then the R wave which has a great amplitude and has a positive polarity and lastly, the S wave, similar to the Q wave but with a slightly higher amplitude. The time interval between two high amplitude R waves (R-R Interval) is used to calculate the instantaneous heart rate. The last wave is the T wave, which is produced by the ventricular repolarization and is similar to the P wave but has a higher amplitude. Between the T and the P wave there is a horizontal line named baseline where there is no electrical activity due to the isoelectric phases of the cardiac cycle. These phases are the diastole and the diastasis, during which all the cells of the heart are polarized. A very small additional wave called the U wave (not shown) is sometimes registered 40ms after the T wave, but it has such a low amplitude that it doesn't appear in most ECG apparatus and although there are no certainties of it, it is believed to be due to slow repolarization of ventricular papillary muscles.

#### 2.4. ECG in sports

This project has been developed around the idea of designing a ECG registration system that is going to be used in sports therefore the importance of ECG monitoring in sports must be stated. Many studies have focused in measuring the ECG in effort tests such as the Cooper test however, the national medical institute also recommends to monitor the sport activities of citizens older than 50 years old to prevent cardiac malfunctions. There have also been tragic cases of sudden cardiac death in sports which could have been detected and prevented with the use of a portable, non-invasive ECG systems that could monitor the athlete as he competes or trains. Applications of an apparatus that would be able to register an ECG without interfering with the

activity would be countless. As this project focuses in the design of such apparatus, some considerations must be taken into account in order to define the specifications. Obviously, the system must be as small as possible and wireless so that people could do sports while carrying them. Unfortunately, due to manufacturing and resources limitations, this could not be accomplished. The least amount of wires should be used and the leads modified. Athletes would not be able to move freely if they have wires connected to their wrists and ankles therefore precordial leads had to be considered. Precordial leads place the exploring electrode directly on the chest as shown in Figure 2-11. Table 2-3 describes the six unipolar standardized precordial leads.



V <sub>1</sub>	4 <sup>th</sup> Intercostal (right)
V <sub>2</sub>	4 <sup>th</sup> Intercostal (left)
V <sub>3</sub>	Between V <sub>2</sub> and V <sub>4</sub>
V <sub>4</sub>	Mid-clavicular (Mid-collarbone)
V <sub>5</sub>	5 <sup>th</sup> Intercostal space (Anterior axillary line)
V <sub>6</sub>	5 <sup>th</sup> Intercostal space (Mid-axillary line)

Table 2-3 – Normal chest leads placements

Figure 2-11 – Normal chest leads. Modified from [10]

It is well known that elite athletes' hearts are bigger and stronger as they perform under high stress and the cardiac muscle, as any muscle, adapts and gains strength. These morphological changes can sometimes result in cardiac pathologies. Changes in cardiac rhythm and frequency and specially sinus bradycardia, a sinus rhythm that is under 60 beats per minute, are the most common alterations detected.

### 3. OBJECTIVES AND JUSTIFICATIONS

#### 3.1. Objectives

The aim of this project is to design and manufacture an ECG device that could be used during sports which will register the signal, filter it accordingly and amplify it until it could be visualized using standard oscilloscopes and to develop a LabView program to visualize the signal and applying digital filters to it.

#### 3.2. Academic Justifications

This project consists in the final 12 ECTS that need to be passed in order to obtain the tittle of Grado en Ingeniería en Tecnologías Industriales of the Universidad Politécnica of Valencia. The objective of this project is to prove the practical and theoretical knowledge obtained throughtout the bachellor. The theoretical knowledge includes the concepts learned in Sistemas Electronicos and Tecnología Electronica as well as in Teoría de Circuitos and Proyectos. Being the concepts of the later those used when elaborating this report.

### 3.3. Technological Justifications

More and more, science is focused in studying the impact of sport in our health. People need to be encouraged to do sports but in elite competitions a heart condition, if unnoticed, could prove fatal. For the past 20 years, businesses and investigators have developed systems that could monitor the athletes as they performed without interfering too much. The system I designed will not only register an ECG but will also be able to visualize and process the signal digitally.

## 4. THEORETICAL BACKGROUND

Before attempting the design of the circuit board, a theoretical study had to be made in order to determine the optimum specifications that the system had to have. This study includes a brief introduction to the characteristics of an ECG signal, the main source of interferences and how to deal with them and the safety requirements that need to be taken into consideration not to endanger the patient which are stated in UNE-EN 60601-2-47 and ANSI/AAMI/IEC 60601-2-24:2011.

### 4.1. Signal characteristics

The standard cardiac signal has defined characteristics that will be considered when designing the ECG registration system. The amplitude and the frequency response of the signal are the features that are going to determine part of the specifications of the system.

As commented before, the amplitude of the signal depends on the standard lead used to measure the ECG. This signal has an amplitude between 1 and 5mV which are values difficult to read in a typical oscilloscope. For this reason, the system was designed to have a gain of 1000. UNE-EN 60601-2-47 clearly states in article 51.5.1 Dynamic entry range, that the system must be able to handle and visualize differential tensions of 6mV peak-to-valley. The system, with a gain of 1000, would develop an output signal of 6V, which being lower than the power supply voltage ( $\pm 9V$ ), would be able to follow what the legislation demands. American National Standard ANSI/AAMI/IEC 60601-2-27:2011 demands only 5mV peak-to-valley in article 201.12.1.101.2 so if the systems follows the UNE legislation so would the ANSI.

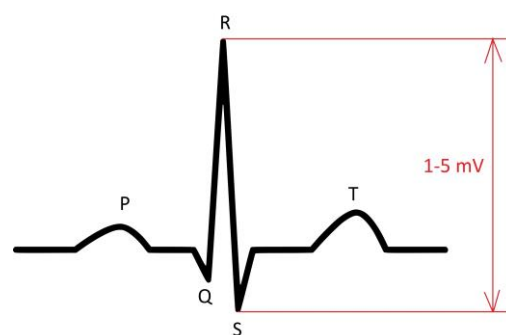


Figure 4-1 – ECG Typical Peak-to-Peak Value. Modified from [9]

In order to design the filters of the system, the frequency spectrum of the ECG must be studied. Figure 4-2 shows the spectrum of a typical ECG signal.

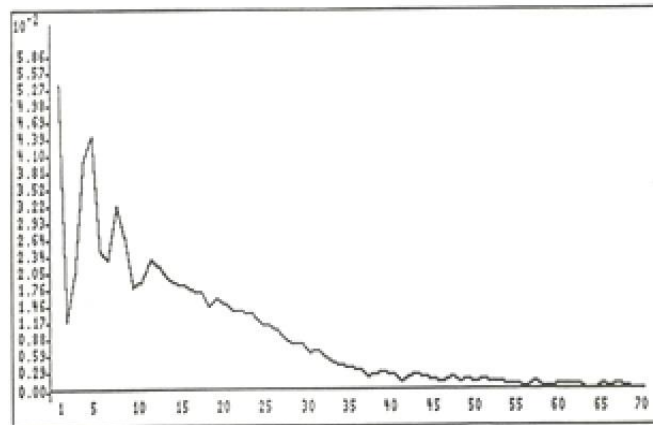


Figure 4-2 – Typical ECG frequency spectrum [8]

The bandwidth of a normal ECG is not very wide and the fundamental frequency is approximately 1 Hz. The harmonic content decreases until is practicably negligible beyond 60Hz however, the system higher cutoff frequency was fixed to be 150Hz as part of the QRS complex is lost if filtered at lower cutoff frequencies. The lower cutoff frequency was fixed at 0.5Hz to eliminate the direct voltage component.

#### 4.2. Interference sources

The study of interference or artifact sources is critical for our project as they get amplified with the signal. The main sources that the system must be partially protected from are the inductive effect of the artifacts induced by the main power grid and the noise generated by the muscles during sports. However, the noise produced by other sources such as other electronic devices used will be taken into account too.

The electric power lines are connected different apparatus, appliances and run inside the walls and floor of the room. These power lines affect the recording of the ECG by introducing interferences at the line frequency (50Hz in Europe) and can appear as the result of two mechanisms, which can affect separately or in most cases, together. One of these mechanisms is the electric field coupling between the power lines and the system or the patient. We could model the system (including the electrocardiograph, patient and electrode wires) and the power lines as two conductors separated by a dielectric substance (air), this results in parasitic capacitances that connect our system to the main grid and to ground, creating a closed circuit and a common mode voltage appears. This is shown in Figure 4-3. Most ECG systems minimize this effect by shielding the leads and grounding each shield at the electrocardiograph. Lowering the skin-electrode impedances is also helpful and will be described in more detail later on.

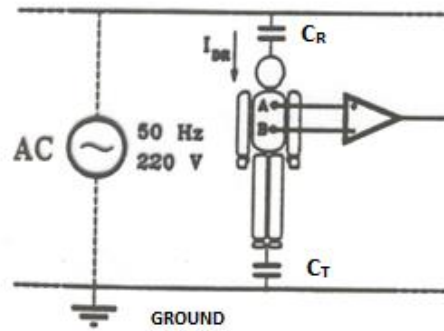


Figure 4-3 – Effect of the main grid in the patient's body [8]

The other source of artifact from the power lines is magnetic inductions. The current flowing through the grid's wires creates a magnetic field. When a magnetic field passes through a coil, like the one produced by the lead wires as shown Figure 4-4 (a), a voltage is induced in this loop. This can be reduced by keeping the system and the wires away from magnetic fields, something which is highly difficult to accomplish, or by unwinding the cables reducing the effective area of the loop as shown in Figure 4-4 (b).

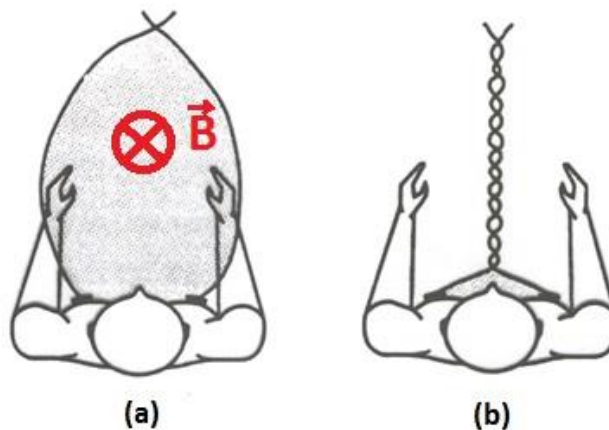


Figure 4-4 – (a) Leads in a loop with a magnetic field going through it.

(b) Intertwined leads. Modified from [8]

The other main source of interference comes from the fact that the system is designed to be used during sports and this obviously involves a certain degree of movement. The muscles in the body contract when excited with electrical impulses, this gets registered by the contact electrode and seems as if the ECG has been affected by random activity. Low amplitude muscle tremors can mimic the baseline and can be subtle however, in normal cases, the wandering baseline effect appears. In wandering baseline, the isoelectric line changes position. One possible cause is the cables moving during the reading. Patient movement, dirty lead wires/electrodes, loose electrodes, and a variety of other things can cause this as well. Figures 4-5 and 4-6 show the standard waveform of muscle activity and wandering baseline separately, though they tend to appear together.

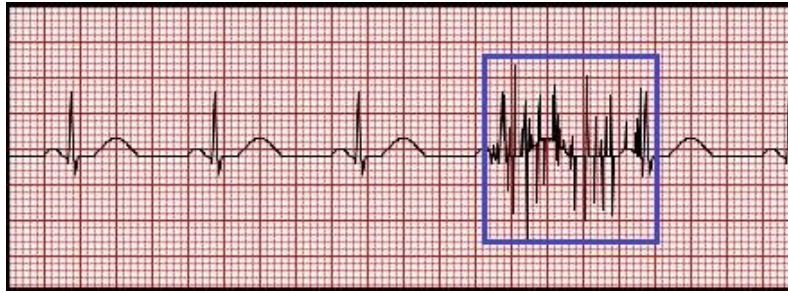


Figure 4-5 – Muscle tremor in ECG [11]



Figure 4-6 – Wandering baseline in ECG [11]

### 4.3. Reduction artifacts techniques

There are various ways of reducing the artifacts described. The earlier mentioned common mode is the main responsible for much of the interference in biopotential amplifiers. European-Spanish Legislation UNE-EN 60601-2-47 states in article 51.5.3 that the minimum common-mode-rejection ratio, hereinafter CMRR, must be 60dB. Although having an amplifier with a high CMRR value would minimize the interferences, there are ways of increasing the CMRR of the system using other approaches, one of which is the driven-right-leg system. This consists in feeding an amplified version of the common mode to the patient in order to reduce the 50Hz interference. A more extensive description of this system will be explained in the Theoretical Design.

### 4.4. Safety requirements

The equipment designed is going to be connected to a patient and has to follow some strict requirements in order to ensure the safety of the patient. The effect of an electric current on a patient depends on: its magnitude (shown in Table 4-1), frequency, type of exposure and place of application (entry and exit points).

Perception	0.5-5 mA
Involuntary Contractions	10 mA
Respiratory Paralysis	20 mA
Ventricular Fbrillation	80-400 mA

Table 4-1 – Effect of electric current depending on its magnitude

The perception values are relatively low but anything above 20mA could be fatal to a patient. The parts which are applied directly to the patient can be classified as Type BF (Body Floating) and Type CF (Cardiac Floating) and each classification has different requirements from the point of view of protection against electrical shock. Type CF is for devices where the applied part is in direct conductive contact with the heart while Type BF is for devices that are in contact with the surface of a patient.

To avoid unwanted currents to flow through the patient's body, an isolation system is used. This system consists in an isolated amplifier and an isolated power supply. The isolation stages create an electrical separation between the patient and the rest of the system, including the power supply and other equipment connected to it such as oscilloscopes. The characteristics of the protection equipment that enable this separation will be commented further on (see 5.3).

#### 4.5. Electrode characteristics

In order to measure and record biopotentials, it is necessary to use electrodes as an interface between the patient and the system. Figure 4-7 shows the system used to model the electrodes, where E1 and E2 are the half-cell potentials (0.1-1V) and Z1 and Z2 the impedance associated with the electrode-skin interface.

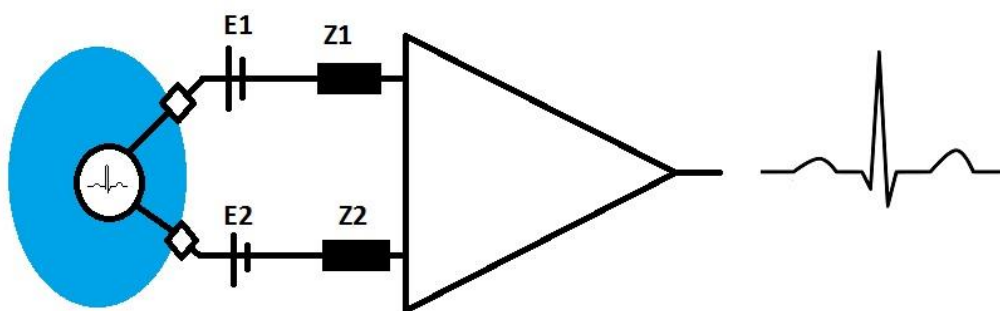


Figure 4-7 – Electrode model

E1 and E2 appear due to RedOx reactions that take place under the skin and affect the system. For them to cancel each other out they need to be exactly equal which is impossible due to the fact that those potentials depend on the contact difference, the impurities present in the skin and even in crystallographic differences between the electrodes. A variable EP is defined as:

$$E_p = |E_1 - E_2| \quad (2)$$

And as:

$$E_1 \approx E_2 \rightarrow |E_1 - E_2| \neq 0 \quad (3)$$

EP is going to be amplified with the rest of the signal so its value should be known beforehand. However, EP depends on the measuring technique so there is no way of knowing its value. The fact that EP is a direct voltage i.e. has frequency of 0Hz, is assumed when designing the specifications of the system. Article 51.5.1 of the UNE-EN 60601-2-47:2001 states that the system must be able to work with the presence of an offset direct voltage of  $\pm 300\text{mV}$  so the

assumption that  $EP=300mV$  was also made when determining the specifications. As mentioned before, there are also interface impedances ( $Z_1$  and  $Z_2$ ) which indicate the willingness of the RedOx reactions to occur. Figure 4-8 shows how the impedances change with frequency. In our case, the frequency is between 1 and 100Hz.

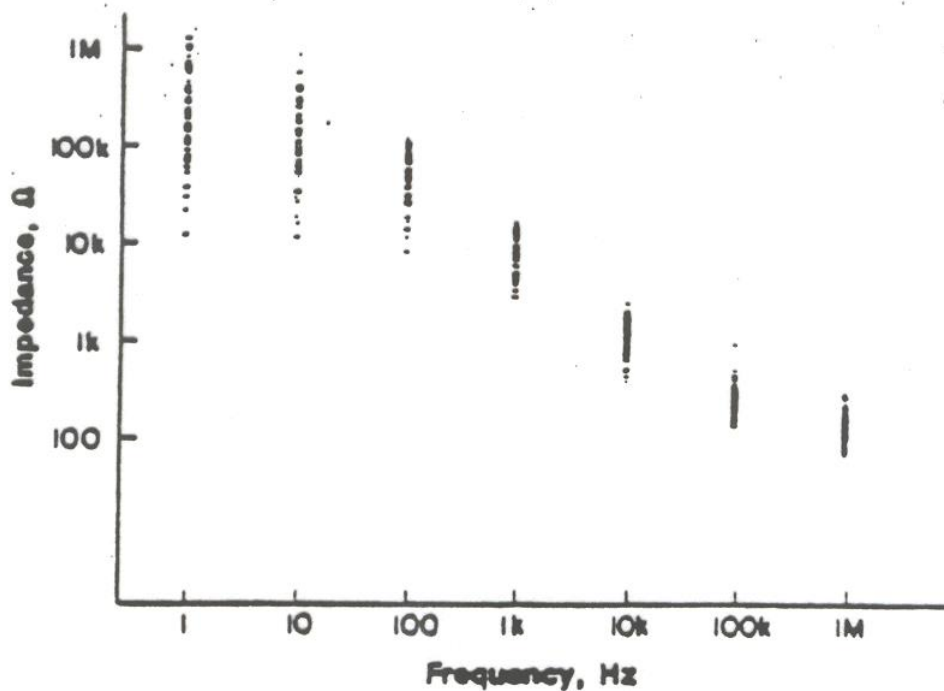


Figure 4-8 – Variation of skin impedance with frequency [12]

The graph shows the effect of the frequency up to 1MHz, but as we have discussed before, the normal frequency of an ECG is 60bpm or 1Hz. This means that  $Z_1$  and  $Z_2$  could have an order of magnitude of  $M\Omega$ . The reason for this is that the epidermis has a very low conductivity, i.e. has a great impedance ( $Z_{epi}$ ) and to reduce this impedance an electrolytic paste is used. Figure 4-9 shows how the ions present in the paste flow through the epidermis creating low impedance passages hence decreasing the total impedance of the system.



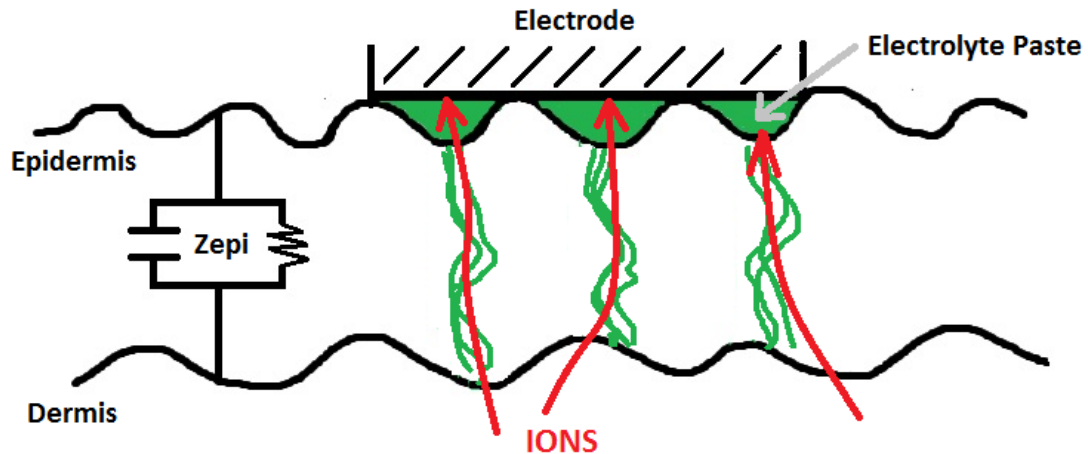


Figure 4-9 – Effect of electrolyte paste in reducing the epidermis' impedance

## 5. DESIGN PROCESS

Following the ideas mentioned in the previous points, the ECG registration device should have a relatively high gain as the ECG normal amplitude is 1-5mV with filters that would attenuate signals below 0.05Hz and above 150Hz and 50Hz if needed. The patient should be properly isolated in order to ensure its safety and the system must be prepared to deal with sudden increases of voltage due to defibrillator shocks. A system for artifact reduction should also be designed.

### 5.1. Specifications

The goal was to design an ECG that would be used during sport activities and therefore the specifications chosen were as follows:

- 1) A total gain of 1000
- 2) A High Pass Filter Cutoff Frequency of 0.05 Hz
- 3) A Low Pass Filter Cutoff Frequency of 150 Hz
- 4) Notch filter for reducing 50Hz interference (operated by the user)
- 5) Common Mode Shield Driver
- 6) Driven-right-leg circuit
- 7) An isolated power supply (DC/DC converter) and an isolated stage to maintain the safety of the patient
- 8) External 9V power supply
- 9) Protection against defibrillator shocks

## 5.2. Block diagram

Taking the specifications under consideration, a block diagram was designed. The diagram shown in figure x consists in several stages. First comes the **instrumental amplifier** and then an **isolation stage** that will maintain the patient separated from any additional equipment connected to the main grid such as an oscilloscope. After the isolation comes the first of the filters, the **high pass filter**, which has the aim of eliminating the direct voltage. The second **amplifier** increases the signal until it reaches the desired gain of 1000. Lastly, the **low pass filter** eliminates the remaining noise. Between the high pass filter and the second amplifier, the user can enable the **notch filter** with the switch. The **isolated power source** supplies the different amplifiers and artifact reduction techniques which include the **common mode shield driver** and the **driven-right-leg circuit** which is connected to the patient.

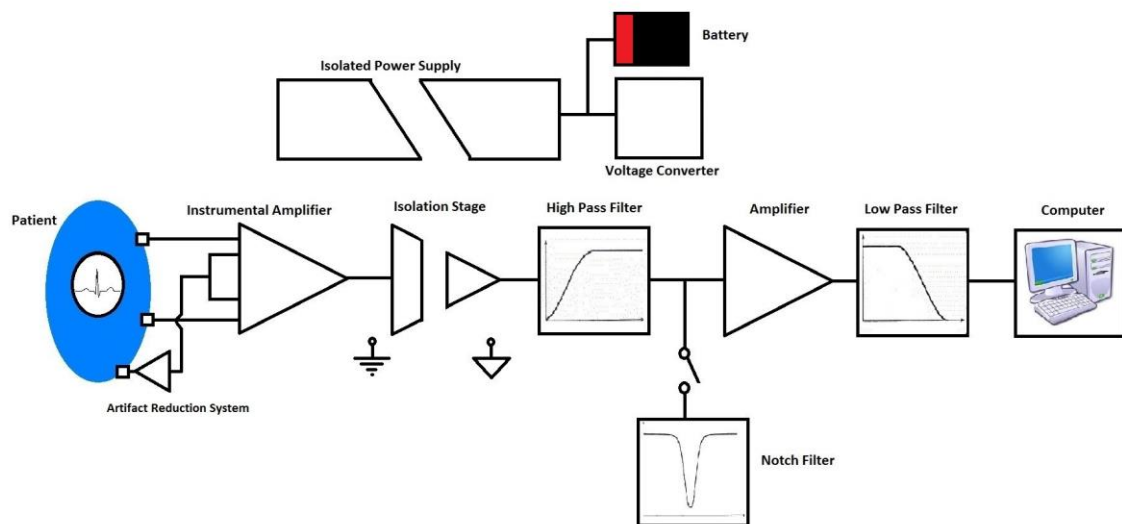


Figure 5-1 – Block Diagram

## 5.3. Theoretical design

The theoretical design was a crucial step when designing the system as the signal that was to be measured has a low peak-to-peak voltage and systems such as this are susceptible to interferences. Throughout the design, batteries of capacitors were used to level out any possible ripples that could be introduced by the power supply needed for the amplifiers. A 10nF capacitor and a 1 $\mu$ F polarised capacitor were used in parallel for every power supply connection consisting in either +9V or -9V. The capacitors improve the power supply rejection ratio or PSRR of the active components of the system. The PSRR is used to describe the amount of noise from a power supply that a particular device can reject.

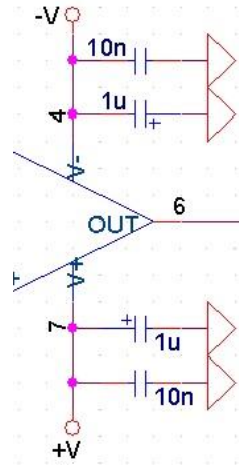


Figure 5-2 – Capacitor Barrier

The OP-AMP used throughout the system are OP27, a precision operational amplifier which combines high speed and low noise (3.5 nV/√Hz).

### 5.3.1. Instrumentation amplifier and equipment protection

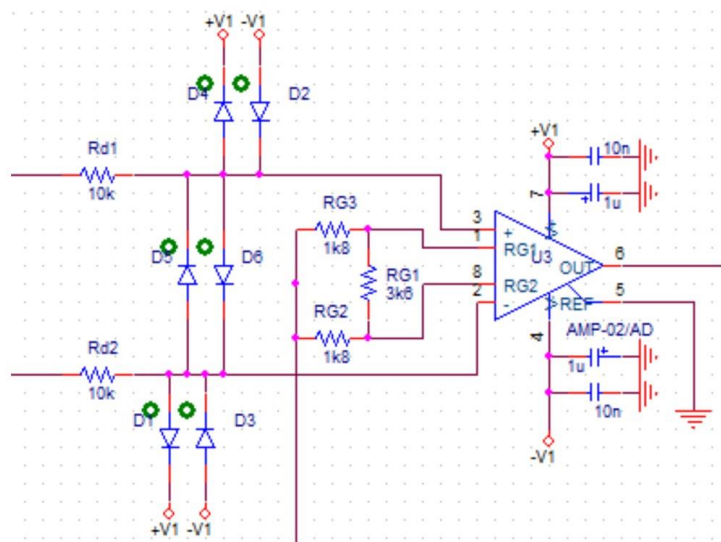


Figure 5-3 – Input Stage

This first stage is critical as the noise will remain in the system and get amplified with the signal and it also has to have a way of protecting the system against sudden increases in voltage that

could be originated by applying a defibrillator to the patient. The defibrillator wave length lasts 4 to 10 milliseconds depending if it has a monophasic or a biphasic waveform. Biphasic defibrillation is widely used and can be attained differently as shown below:

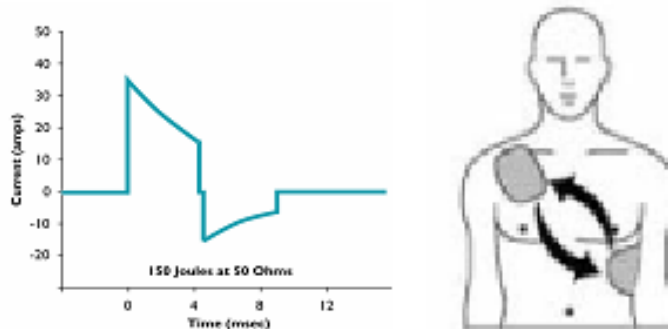


Figure 5-1 – Defibrillator wavelength and application points. Modified from [13]

As can be seen, the defibrillator develops 150 Joules of power but the assumption that no more than 200V will actually reach the system is made.

A mesh of diodes (0,5 Watts) was used for this purpose and according to the specifications of the diodes (See Annexed CD), the current through them must be limited to 20mA. Rd resistances are used to limit this current and the equation used was:

$$R_d = \frac{V}{I} = \frac{200V}{20mA} = 10k\Omega \quad (4)$$

After determining the protection of the system, the gain of the instrumental amplifier had to be evaluated. The instrumental amplifier chosen was the AMP-02, which has a transfer function given by:

$$V_S = G_1(V_2 - V_1) \quad (5)$$

where the gain is:

$$G_1 = \left( \frac{50k\Omega}{R_G} \right) + 1 \quad (6)$$

Being  $R_G$  the equivalent resistance of  $R_{G1}$ ,  $R_{G2}$  and  $R_{G3}$ .

$$R_G = \frac{R_{G1}(R_{G2} + R_{G3})}{R_{G1} + R_{G2} + R_{G3}} \quad (7)$$



To avoid saturation and assuming the maximal voltage in standard conditions is  $E_p=300\text{mV}$ , the gain of the instrumental amplifier was limited to:

$$G_1 = \frac{V_+}{E_p} = \frac{9\text{V}}{0.3\text{V}} = 30 \quad (8)$$

Limiting the gain to 30 would have proven a mistake as the system would be very near the non-linear zone, therefore a gain of 26 was chosen. This meant that the  $R_G$  would be:

$$R_G = \left( \frac{50\text{k}\Omega}{G_1 - 1} \right) = \left( \frac{50\text{k}\Omega}{26 - 1} \right) = 2\text{k}\Omega \quad (9)$$

Which looking at the 1% resistance chart:  $R_G=1\text{k}\Omega$  and therefore, making  $R_{G2}=R_{G3}$ ,  $R_{G1}=3\text{k}\Omega$  and  $R_{G2}=R_{G3}=1\text{k}\Omega$ . The theoretical gain of the instrumental amplifier is:

$$G_1 = \left( \frac{50\text{k}\Omega}{1.8\text{k}\Omega} \right) + 1 = 28.8 \quad (10)$$

To sum things up, this input stage consists of:

- 6 1N4148 diodes (0.5W)
- 1 AMP02
- 2  $R=10\text{k}\Omega$
- 1  $R=3.6\text{k}\Omega$
- 2  $R=1.8\text{k}\Omega$
- 2 Batteries of capacitors (one for each power supply)

### 5.3.2. Isolation stage

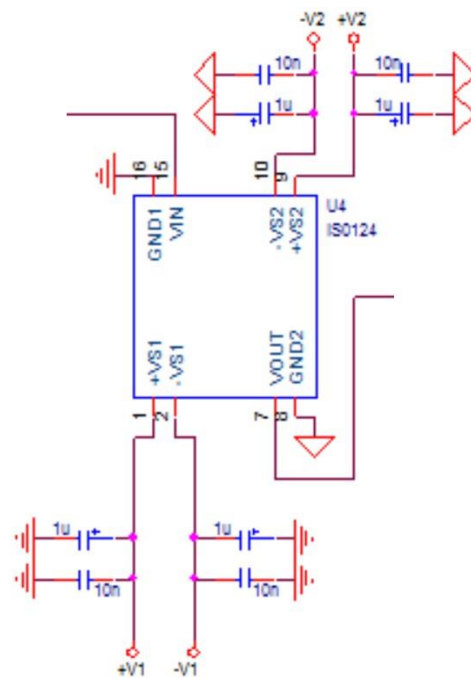


Figure 5-4 – Isolation Stage

This stage provides a physical separation between the patient and the power supply but serves as a bridge which enables the signal to travel through a 2pF capacitive barrier. The ISO124 has a unitary gain so the signal is not amplified as it passes through but has a maximum leakage current at 60 Hz of 0.5  $\mu$ A and a barrier impedance of  $10^{14}\Omega$  (at 60Hz) which makes it adequate for guarantying the patient's safety. It also has a maximal nonlinearity coefficient of  $\pm 0.01$  %FSR. This is the peak deviation of the output voltage from the best-fit straight line expressed as the percentage of ratio of deviation to FSR. As can be observed in Figure x, each side is connected to different masses keeping both sides truly isolated. To ensure the isolation, a physical separation of 3mm was made between the two masses in the board.

This isolation stage consists of:

- 1 ISO124
- 4 Batteries of capacitors

### 5.3.3. High Pass Filter

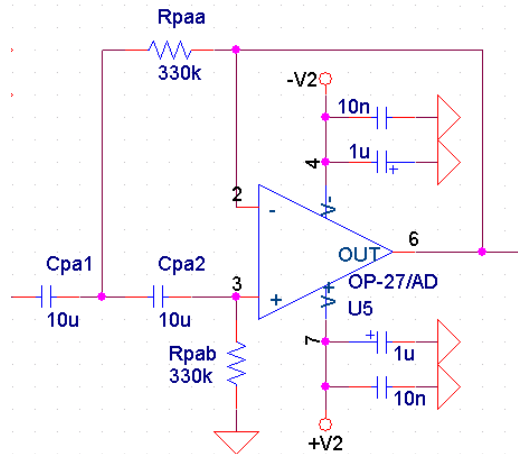


Figure 5-5 – High pass filter

The second-order high pass filter chosen was a Butterworth with a cutoff frequency of 0.05Hz. The cutoff frequency is considered to be the frequency at which 70% of the signal remains unaltered or when the gain in dB is equal to -3dB. The function of this filter is to eliminate the direct voltage present in the signal, a voltage that could be equal to 300mV and if compared against the 1mV peak-to-peak signal and then amplified would make the signal impossible to visualise. The transfer function of a second-order high pass filter is:

$$H(s) = \frac{s^2}{s^2 + 2\zeta\omega_n s + \omega_n^2} \quad (11)$$

where  $s$  is the Laplace operator,  $\omega_n$  the natural frequency ( $\omega_n = 2\pi f$ ) and  $\zeta$  the damping ratio. The equation used to determine the values of the resistances and the capacitors to fix a cutoff frequency of 0.05Hz derived from the transfer function was:

$$f_c = \frac{1}{2\pi CR} = 0.05\text{Hz} \quad (12)$$

The value of the capacitors was chosen to be 10 $\mu$ F therefore the value of the resistances were:

$$R_{paa} = R_{pab} = \frac{1}{2\pi C f} = \frac{1}{2\pi * 10 * 10^{-6} * 0.05} = 318.3\text{k}\Omega \quad (13)$$

which when normalized were  $R_{paa} = R_{pab} = 330\text{k}$ . This filter has unitary passband gain. The theoretical ideal frequency response graph characteristic of a high pass filter is:

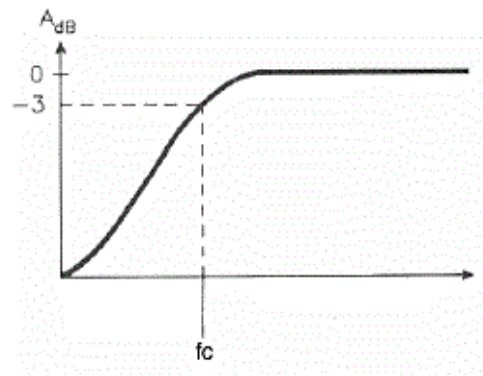


Figure 5-6 – Typical High Pass Filter frequency response. Modified from [14]

The high pass filter stage consists of:

- 1 OP27
- 2 C=10μF
- 2 R=330kΩ
- 2 Batteries of capacitors

#### 5.3.4. Amplifier

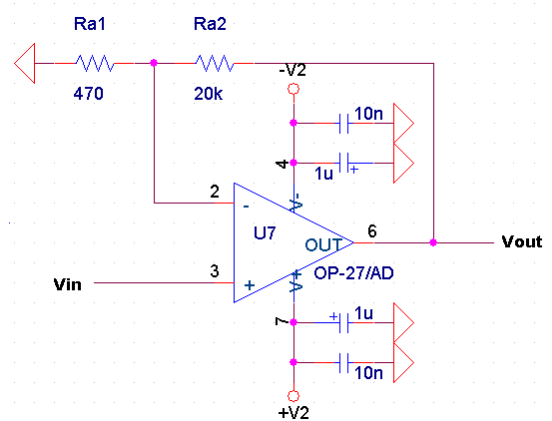


Figure 5-7 - Amplifier

Once the direct current is eliminated, the signal must be amplified again. This amplifier was designed to have a gain of 41 and its transfer function is:

$$V_{out} = G_2 V_{in} \quad (14)$$

The equation that relates the values of the resistances needed with the gain to be obtained was:

$$G_2 = 1 + \frac{R_{a2}}{R_{a1}} = 41 \quad (15)$$



There were an infinite number of values for the resistances that would ensure a gain of 41 in this amplifier. However, in order to reduce the internal noise associated to high values of resistances it is convenient to use low resistance values. Thereby, the values chosen were  $R_{a2}=20k$  and  $R_{a1}=500\Omega$  which ultimately was normalized to  $R_{a1}=470\Omega$ . The final gain for the amplifier was:

$$G_2 = 1 + \frac{20 * 10^3}{470} = 43.6 \quad (16)$$

The total gain desired for this system was 1000 and the gain obtained is:

$$G_T = G_1 * G_2 = 1255.7 \quad (17)$$

It is easy to observe that this first specification was theoretically accomplished.

This amplification stage consists of:

- 1 OP27
- 1 R=470 $\Omega$
- 1 R=20k $\Omega$
- 2 Batteries of capacitors

### 5.3.5. Low Pass Filter

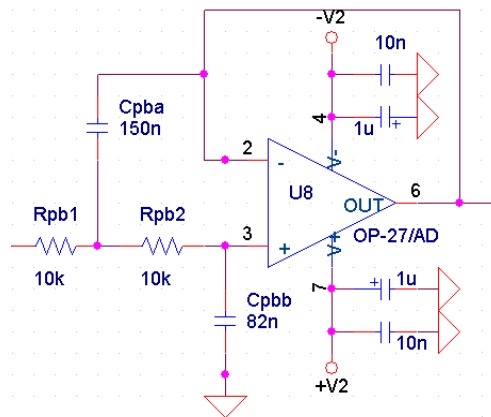


Figure 5-8 – Low Pass Filter

The high frequencies that the signal could have picked up in form of noise and interferences must be eliminated and for this reason a 2<sup>nd</sup> Order Butterworth low pass filter with cutoff frequency at 150Hz was added to the system. The transfer function of this filter is:

$$H(s) = \frac{\omega_n^2}{s^2 + 2\zeta\omega_n s + \omega_n^2} \quad (18)$$

The values of the resistances of the filter were fixed at 10k $\Omega$  and the value of the capacitors were obtained using the following equations derived from the low pass filter transfer function:

$$C_{pba} = \frac{1.4142}{2\pi f_c R_{pb}} = \frac{1.4142}{2\pi * 150 * 10 * 10^3} = 150nF \quad (19)$$

$$C_{pbb} = \frac{0.7071}{2\pi f_c R_{pb}} = \frac{0.7071}{2\pi * 150 * 10 * 10^3} = 75nF \quad (20)$$

The value of  $C_{pba}$  was already normalised but the value of  $C_{pbb}$  was changed to 82nF. The low pass filter has also a characteristic ideal frequency response graph shown in Figure 5-9.

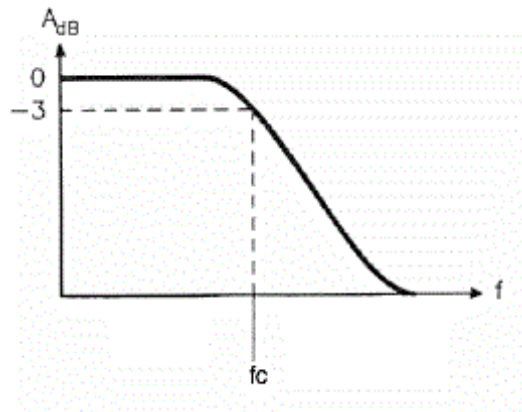


Figure 5-9 – Typical Low Pass Filter frequency response. Modified from [14]

This stage consists of:

- 1 OP27
- 2 R=10kΩ
- 1 C=150nF
- 1 C=82nF
- 2 Batteries of capacitors

### 5.3.6. Notch Filter

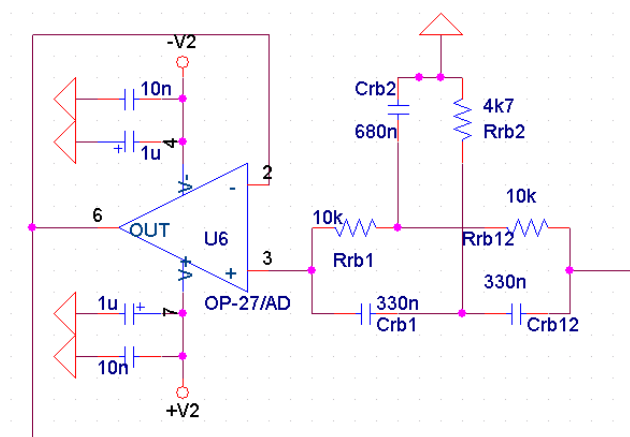


Figure 5-10 – Notch Filter



The band-stop filter or notch filter is designed to cancel the 50 Hz signal introduced by the electric grid. This filter is introduced with a switch that will allow the user to connect or disconnect this filter when visualising the signal as although a main part of the noise present in our signal is eliminated, our signal gets damped as the band-stop filter reduces the passband range of our system. The design of this filter was more complex as it has more components. The transfer function of a second order notch filter is:

$$H(s) = \frac{s^2 + w_n^2}{s^2 + 2\zeta w_n s + w_n^2} \quad (21)$$

The equations that determined the values of the capacitors and the resistances were:

$$f = \frac{1}{2\pi CR} \quad (22)$$

Where C and R could be  $C_{rb1}$  and  $R_{rb1}$  or  $C_{rb2}$  and  $R_{rb2}$  respectively with the particularity that:

$$C_{rb2} = 2C_{rb1} \quad (23)$$

$$R_{rb2} = \frac{1}{2}R_{rb1} \quad (24)$$

Taking this into consideration, the values of the components were chosen and normalized to be as follow:

- $C_{rb1} = 300\text{nF} \approx 330\text{nF}$
- $R_{rb1} = 10\text{k}\Omega$
- $C_{rb2} = 600\text{nF} \approx 680\text{nF}$
- $R_{rb2} = 5\text{k}\Omega \approx 4.7\text{k}\Omega$

With these values we get elimination at:

$$f_{C1} = \frac{1}{2\pi C_{rb1} R_{rb1}} = \frac{1}{2 * \pi * 330 * 10^{-9} * 10 * 10^3} = 48.2\text{Hz} \quad (25)$$

$$f_{C2} = \frac{1}{2\pi C_{rb2} R_{rb2}} = \frac{1}{2 * \pi * 680 * 10^{-9} * 5 * 10^3} = 46.8\text{Hz} \quad (26)$$

The standard notch filter has a characteristic frequency response and the quality of the filter comes determined by the Q coefficient which represents how narrow the notch is. This coefficient depends greatly on the quality of the materials and the components used as well as on the manufacturing technique used and has the following characteristic frequency response:

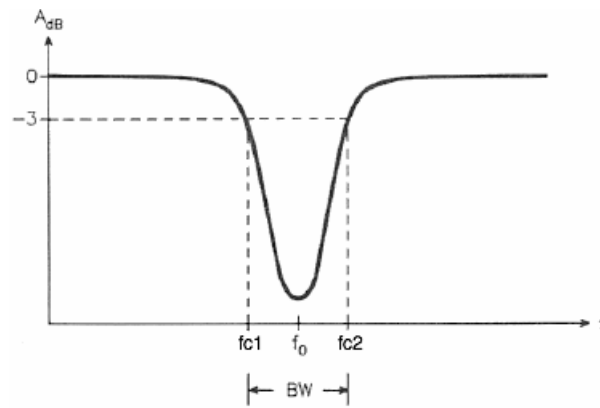


Figure 5-11 – Typical Notch Filter frequency response [14]

The switch used is an ESB33 vertical switch designed to commute between two stages: normal stage (with no 50Hz filter) and 50Hz filter stage in line. This component has an schematic diagram shown in Figure 5-12 and Figure 5-13 shows how the switch changes between both stages.

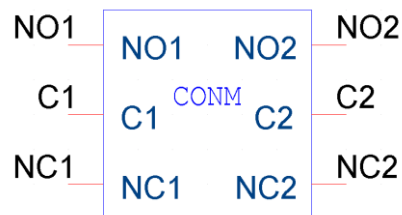


Figure 5-12 – Switch schematic

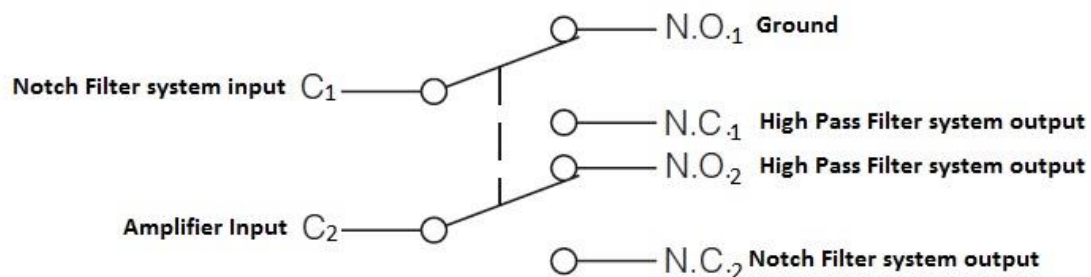


Figure 5-13 – Switch Inner diagram and connections.

This stage consists of:

- 1 OP27
- 1 ESB33 Switch
- 2 R=10k $\Omega$
- 1 R=4.7k $\Omega$
- 2 C=330nF
- 1 C=680nF
- 2 Batteries of capacitors

### 5.3.7. Common Mode Shield Driver

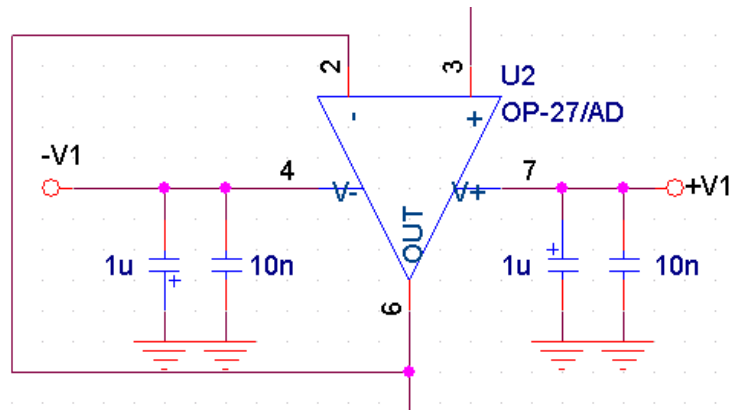


Figure 5-14 – Common Mode Shield Driver

This stage belongs to the early stages of our system and links the instrumental amplifier with the Driven Right Leg, hereinafter DRL, that is then connected to the patient through the 3<sup>rd</sup> electrode. This amplifier has unitary gain and infinite passband range. At its output we can measure the common mode signal. This stage in addition with the DRL are crucial for our system as they both have the mission of reducing the interferences and providing an alternative path to the polarization currents which help the system stabilize. Figure 5-15 shows how this shielding was accomplished.

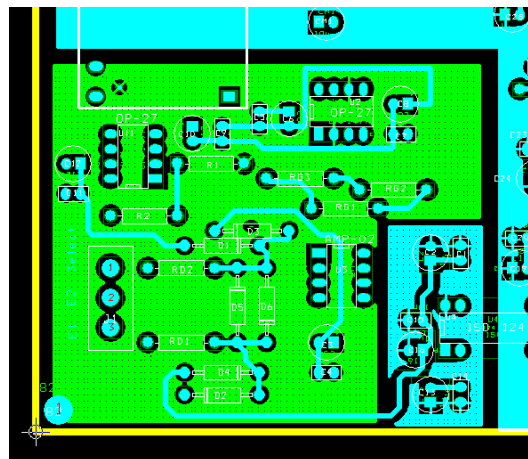


Figure 5-15 – Zoom in section of the Layout (see 5.1) were the shielding is coloured green

This stage consists of:

- 1 OP27
- 2 Batteries of capacitors

### 5.3.8. Driven Right Leg

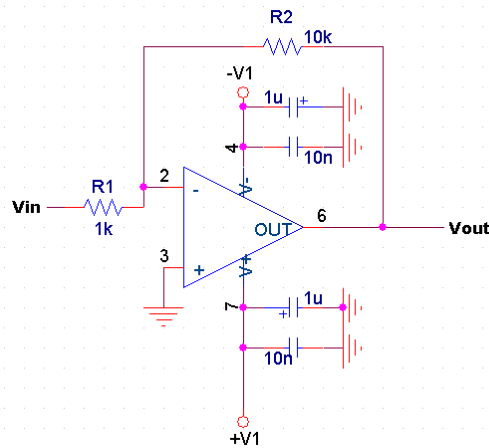


Figure 5-16 – Driven Right Leg

The DRL is an inverter operational amplifier with a gain of -10 that is connected to the patient via the 3<sup>rd</sup> electrode. As commented before, this stage reduces the common mode effect and the value of its resistances was obtained using the following equation:

$$G = -\frac{R_2}{R_1} = -10 \quad (27)$$

The values chosen for the resistances of this amplifier were  $R_1=1k\Omega$  and  $R_2=10k\Omega$ .

This stage consists of:

- 1 OP27
- 1 R=1k $\Omega$
- 1 R=10k $\Omega$
- 2 Batteries of capacitors

### 5.3.9. Isolated Power Supply

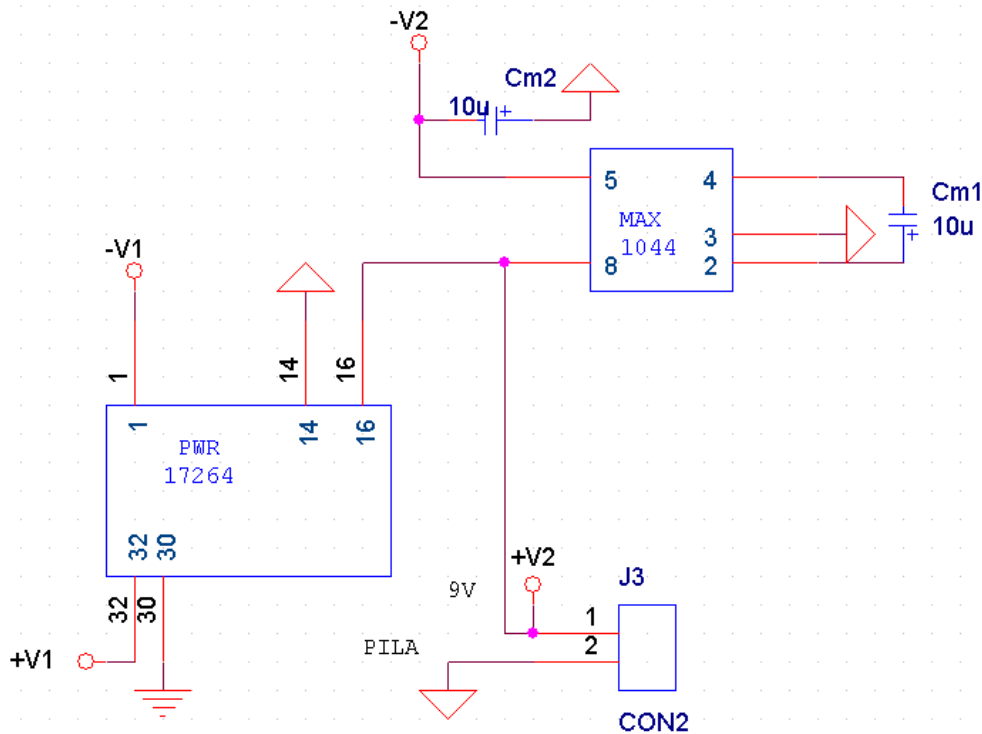


Figure 5-17 – Isolated Power Supply

The isolated power supply consists in two distinct components: the PWR17264 and the MAX1044. The power source that was used is a 9V alkaline battery that was firstly connected to the MAX1044, a switched-capacitor voltage converted which had the aim of producing the negative voltage power supply that the operational amplifiers need. While this was accomplished, the PWR17264, a 1.5 Watt unregulated DC/DC converter produced the second set of power supplies referred to a different mass. By doing so, both isolated circuits were supplied and the system was ready to function. The MAX1044 has 2 polarized 10 $\mu$ F capacitors that smooth out the possible ripples that could be found in the power supply. The PWR17264 has a high isolation voltage of 3500 V<sub>rms</sub> and a maximal leakage current of 2  $\mu$ A.

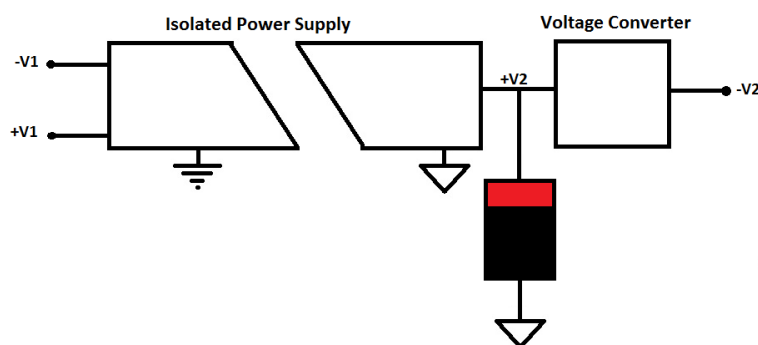


Figure 5-18 – Isolated power supply block diagram

The isolation stage consists of:

- 1 MAX1044
- 1 PWR17264
- 2 Polarized C=10 $\mu$ F
- 1 9V Battery

## 6. CIRCUIT DEVELOPMENT

### 6.1. OrCAD Capture and Layout

Once the theoretical design was finished, the circuit had to be manufactured and to do so, first a schematic diagram had to be drawn and then a final layout had to be developed. The OrCAD program with Capture and Layout features were used for this stage. OrCAD version 16.0 was used as the UPV has an educational license for the program.

OrCAD Capture was used to have a clear idea of how the different stages would interact with one and other. The schematic was useful when designing the layout and during the welding process in order to remember the value of the resistances and the capacitors of each stage. Figure 6-1 shows the program's main window where the schematic was drawn as well as the Place Part tool that was used to insert the components.

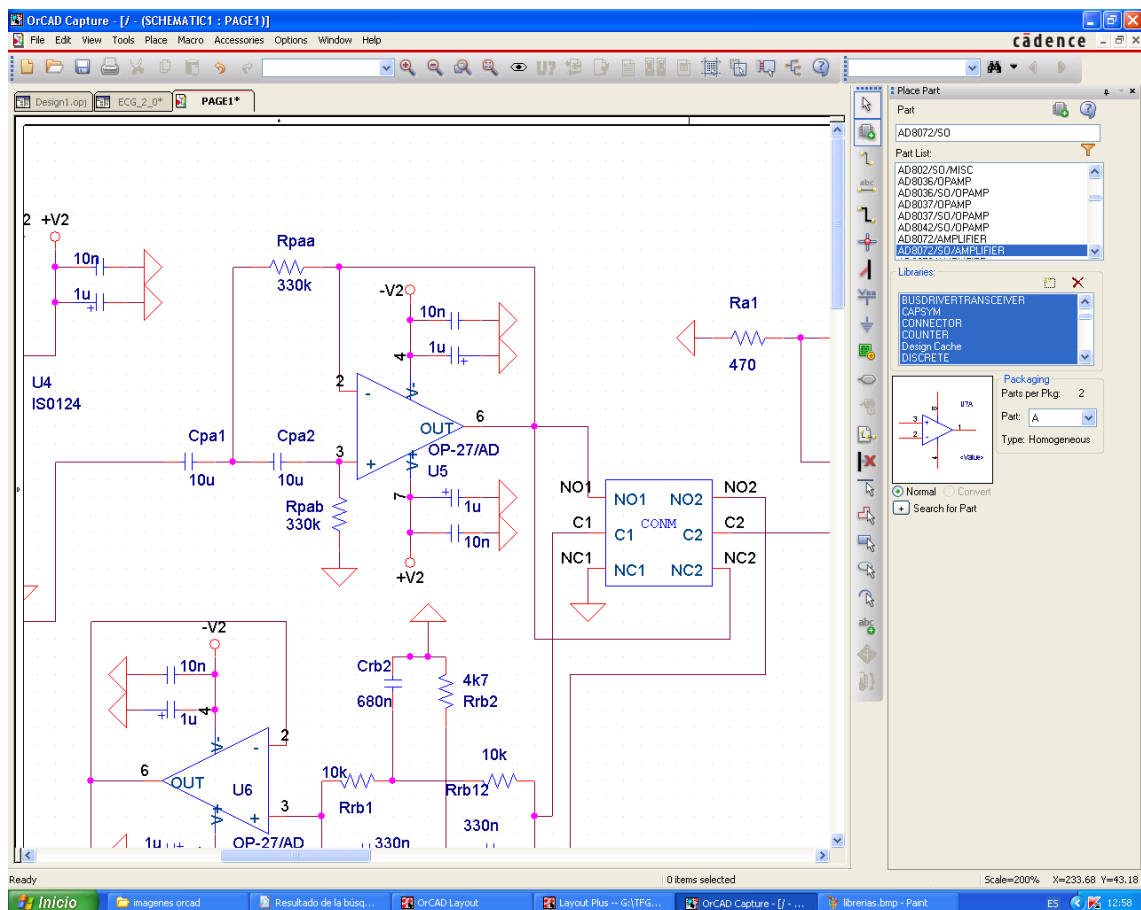


Figure 6-1 – OrCAD Capture interface



The components had to be found in the various built in libraries the OrCAD provides. However, some of the more specific components such as the switch, the PWR and the MAX had to be designed with the footprint tool Capture offers and saved to my personal library LIBRARY1.

The different libraries used are listed in Figure 6-2.

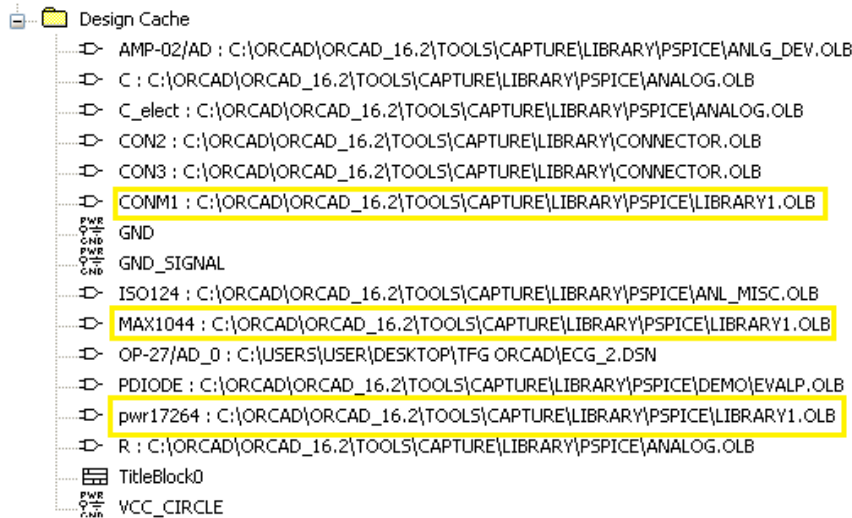


Figure 6-2 - Libraries

The final template that would then be printed and used to manufacture the circuit was designed using the OrCAD Layout. OrCAD is able to use an existing Capture file to create a new Layout file, by doing this, all of our components would automatically appear in the Layout file. Figure 6-3 shows the interface of the Layout, note that the components are already in their final position.

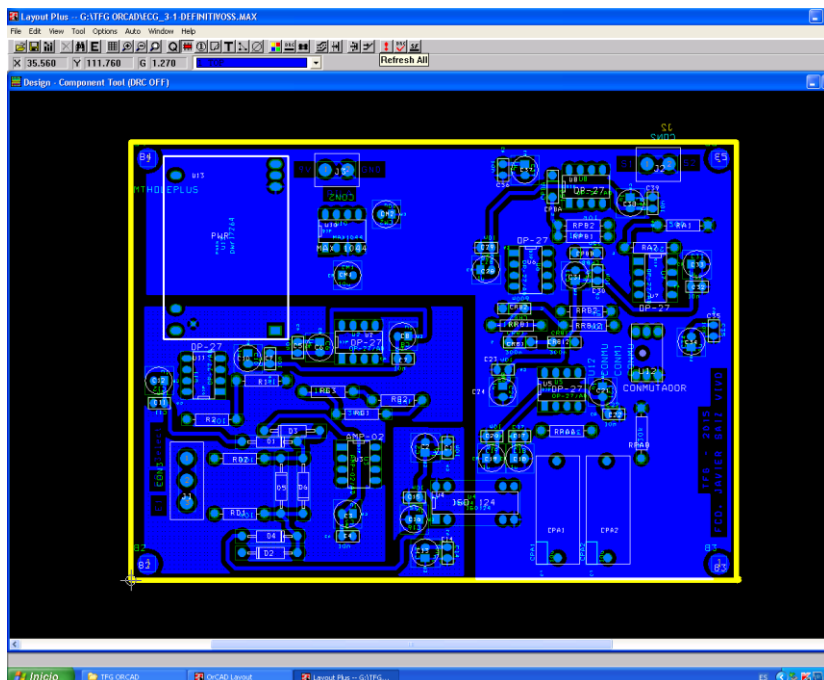


Figure 6-3 – OrCAD Layout interface

For the transfer from Capture to Layout to be done properly, each component in the Capture file should have been linked to an existing footprint. Most of our components had virtual representations in internal libraries such as resistances and the DIP8 used for the operational amplifiers but for some components, a new footprint had to be created or modified. Figure 6-4 shows the Library Manager to design were the footpaths could be created and edited, more specifically, an already created DIP8S was modified

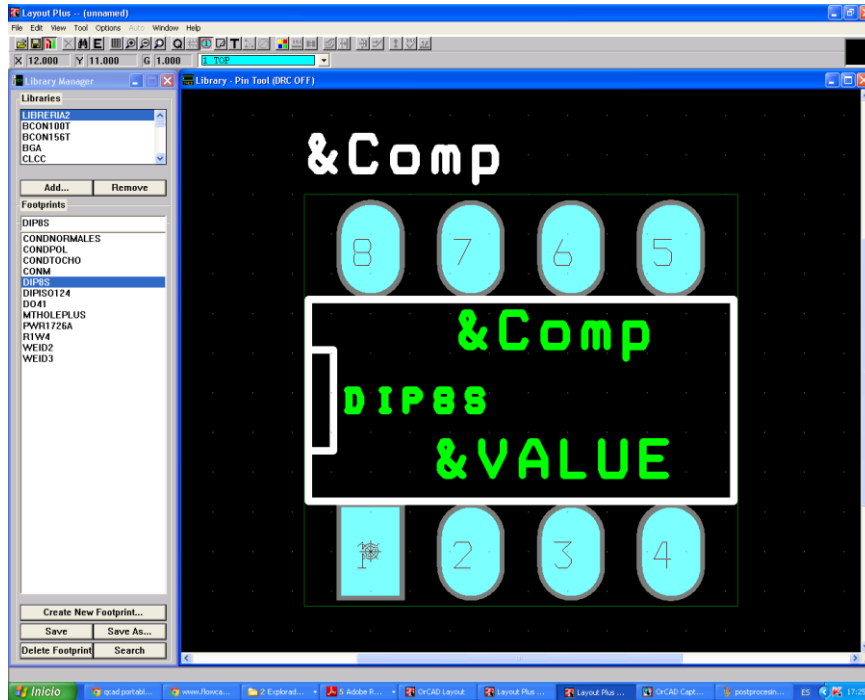


Figure 6-4 – Library Manager

After considering the limitations of the manufacturing process, every footprint was modified to have bigger pads. The pads are where the component is to be welded and during the manufacturing process, when doing the drilling for the component to be inserted, small pads could easily be drilled off. The pads differ from component to component but an example of the pad dimensions used for the oblong pads in the DIP8 are shown in mm in Table 6-1– Padstack dimensions

Padstack or Layer Name	Pad Shape	Pad Width	Pad Height	X Offset	Y Offset
TOP	Oblong	1.473	2.235	0.000	0.000
BOTTOM	Oblong	1.473	2.235	0.000	0.000
PLANE	Oblong	1.727	2.489	0.000	0.000

Table 6-1– Padstack dimensions

For the manufacturing process to be done successfully other characteristics had to be determined. This was very important as the chemical attack process is not very accurate and some tracks could be eaten off.

Track to Track	Track to Via	Track to Pad	Via to Via	Via to Pad	Pad to Pad
0.254	0.254	0.254	0.254	0.254	0.254

Table 6-1 – Forced distances in Layout

Table 6-1 shows the average distances measured in mm that could be enforced in the Layout file in order to ensure a correct manufacturing process. Once the layout is finished, the transparency is printed and the manufacturing process begins.

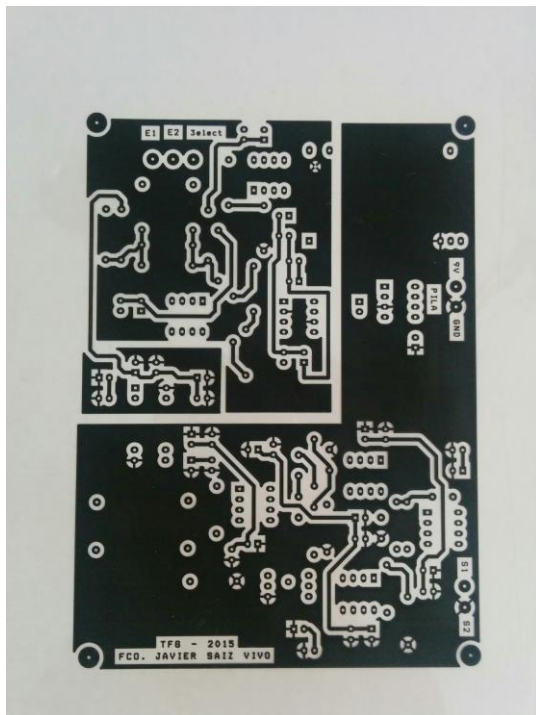


Figure 6-5 – Top transparency

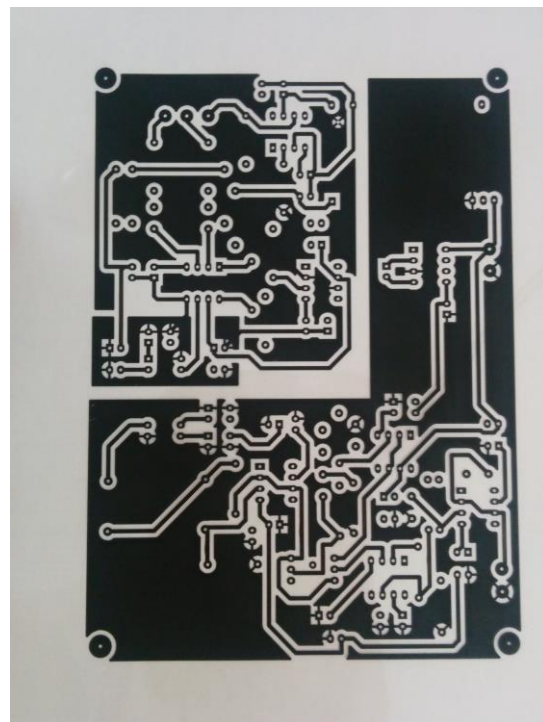


Figure 6-6 – Bottom transparency

The images show the final transparencies used in the manufacturing process. Figure 6-5 is the front and Figure 6-6 is the back.

OrCAD enabled us to save the whole project a series of files called Gerbers that contain everything a factory may need to manufacture our product. The Gerber File is part of the annexes present in the CD and will be fully described in the Statement of Specifications.

## 6.2. Manufacturing Process

The manufacturing process had some limitations and although the technique used had its drawbacks and was not very accurate, we succeeded in manufacturing the board. The manufacturing process held 4 different processes: insulation, chemical attack, machining and soldering. First, in the insulation process and once the schematic transparency was printed, the presensitized circuit board was exposed to UV light for 100s with a double layer contact printer.

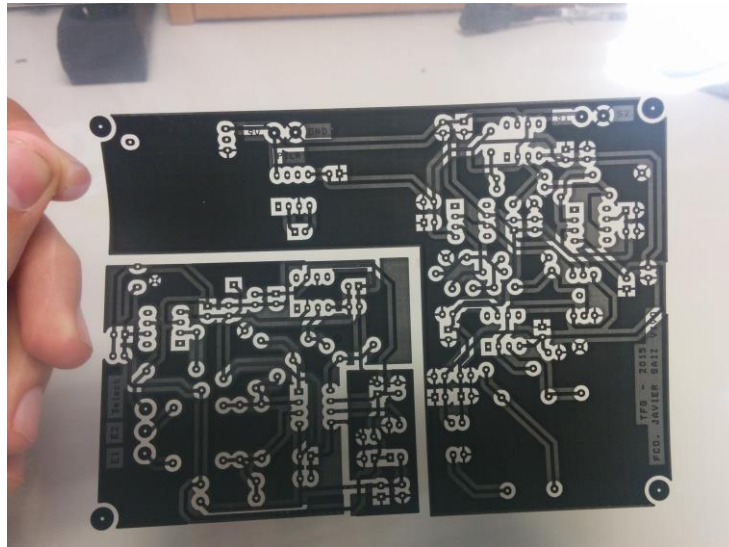


Figure 6-7 – Both transparencies combined



Figure 6-8 – UV light exposition process

Figure 6-7 shows both transparencies combined. The drill holes had to be perfectly aligned so that they could be drilled properly. In Figure 6-8 the insulation process can be seen.

The board is covered in photoresist which when exposed to light will decay and the copper underneath will be revealed. Next comes the chemical attack. Once the exposure has finished, the transparency was removed and the board was introduced into a Maquina de atacado MEGA

where the copper that was exposed and the remaining of the photoresist will be eaten away. The chemical attack consists in 2 phases: firstly there is a photographic processing where the board is submerged into a solution of water and caustic soda, then comes the chemical attack where the board is treated with iron chloride until the remaining unwanted copper is eliminated. Precautions must be taken as if the board remains too long in the chemical solution, some of the copper tracks or pads could also be eliminated.



Figure 6-9 – Photographic processing



Figure 6-10 – Chemical Attack

The figures show how the chemical attack was made. As can be observed in Figure 6-10, the board is starting to look as an actual circuit board. The next images show the board once taken out of the chemical bath and once cleaned with acetone and the excess photoresist washed off.



Figure 6-111 – Board after chemical bath

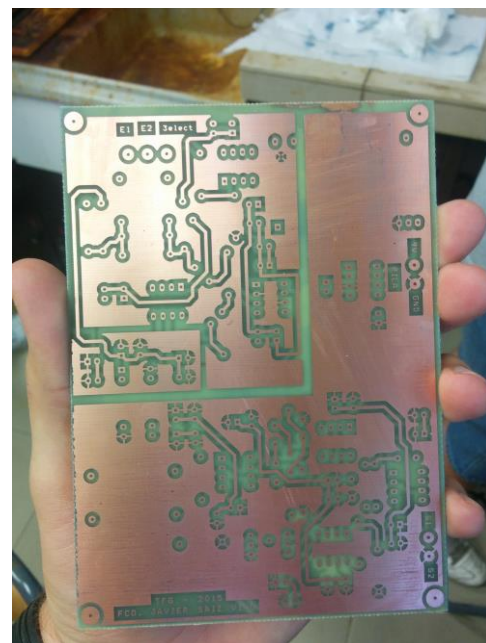


Figure 6-122 – Board rinsed

After the board was rinsed, the drilling process started. A 0.75 mm drill was used for the pads of the components whereas a 1 mm drill was used for the connector's pads and a 3.5 mm one for the 4 supporting screws. The following images show the drilling process as well as the final result.

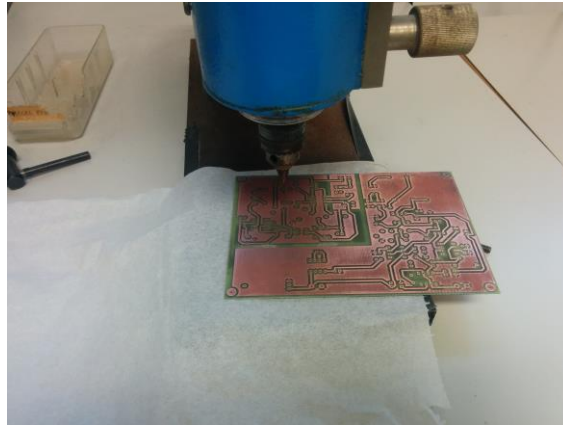


Figure 6-13 – Board with drill



Figure 6-14 – Board being drilled

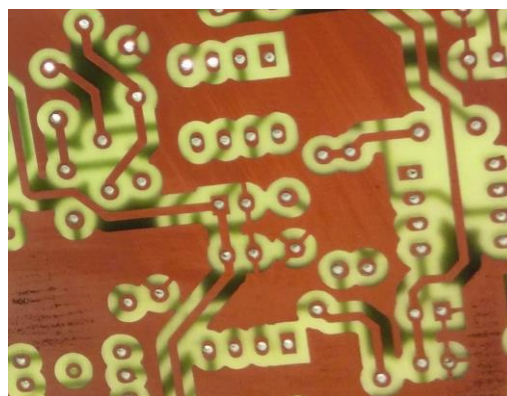


Figure 6-15 – Board with the holes drilled

The last part of the manufacturing process was the soldering of the components. This process was crucial as any soldering defect could mean a bad connection and therefore a source of error or even the reason the system wouldn't operate as expected. Some of the more expensive components such as the PWR or the ISO124 were not soldered directly to the board. Plug-in sockets were used to introduce these components to the system.



Figure 6-16 – Finished Circuit Board

## 7. TESTS AND RESULTS

### 7.1. Frequency Response

The frequency response is going to be evaluated with and without the 50Hz filter so that we can discuss why although the filter cancels the 50Hz effect of the main grid, if it doesn't interfere too much, is best not to have it active.

#### 7.1.1. Frequency response without the 50Hz Filter

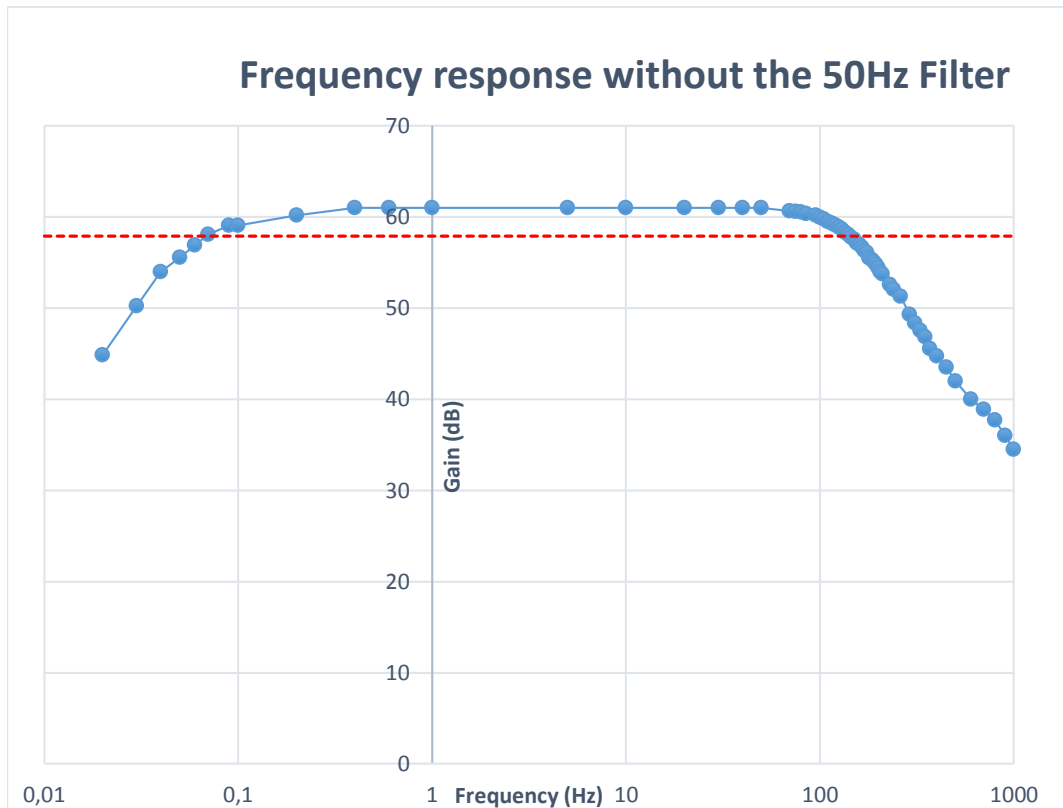


Figure 7-1 – Frequency response without the 50Hz Filter

A frequency response test was made to check if the system met the desired specifications. As can be seen, the graph shows a band-pass filter frequency response which is what one obtains when combining a high pass filter with a low pass filter. The graph shows the dependence of the gain of the system in dB to the frequency in Hz. The passband gain is 61dB which is equivalent to an absolute gain of 1120. The red line indicates where the cutoff frequency lies within the graph. It is the 70% of the absolute gain or a reduction of 3dB from the gain in dB. Although the filters were designed to have a lower cutoff frequency at 0.05 Hz and a higher cutoff frequency at 150 Hz, this test shows that the system has the cutoff frequencies at 0.07Hz and 143.3Hz. We have a higher gain but a thinner passband region than expected. This phenomenon must be due to the tolerances of the components and the effect the normalizations had on the theoretical calculations made.



### 7.1.2. Frequency response with the 50Hz Filter

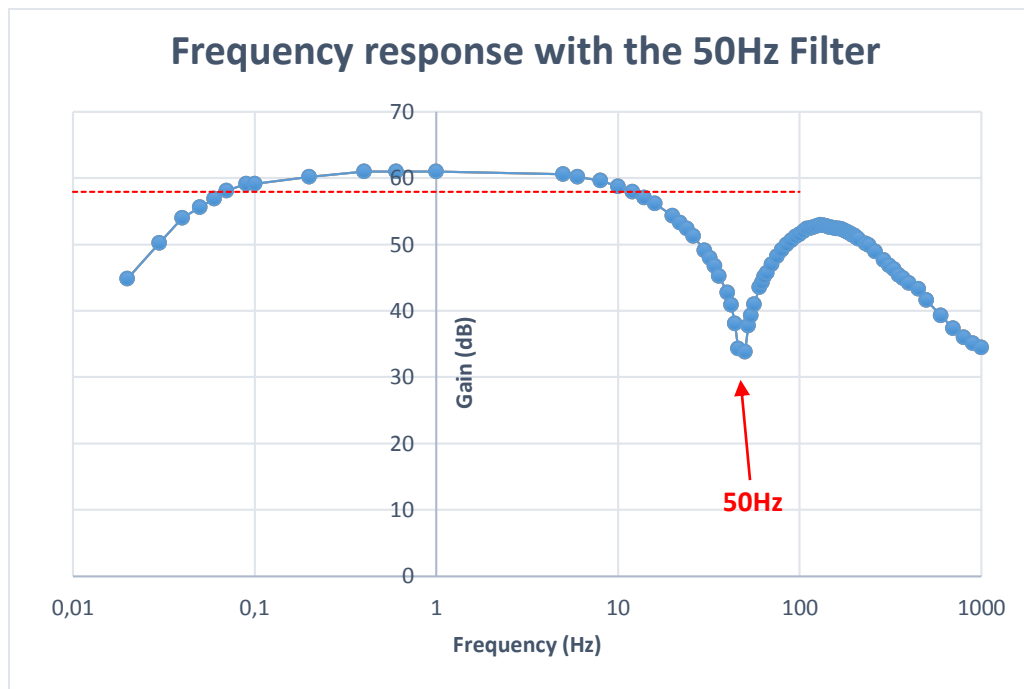


Figure 7-2 – Frequency response with the 50Hz Filter

When the 50Hz filter is applied there is a distinct effect on the frequency response. For lower frequencies there is no significant change but when approaching 50Hz the absolute gain of the system decreases from 1120 to 49. This means a reduction of 95.6% of our passband gain which ultimately signifies that the 50Hz component of the signal created by the parasitic effect of the main grid gets nearly completely eliminated. Having such a hard reduction has a side effect. As can be observed in the figure, after the notch in 50Hz the gain is not able to return to its passband value before decreasing again so parts of useful information contained in the signal could be lost.

## 7.2. Rejection of the common mode

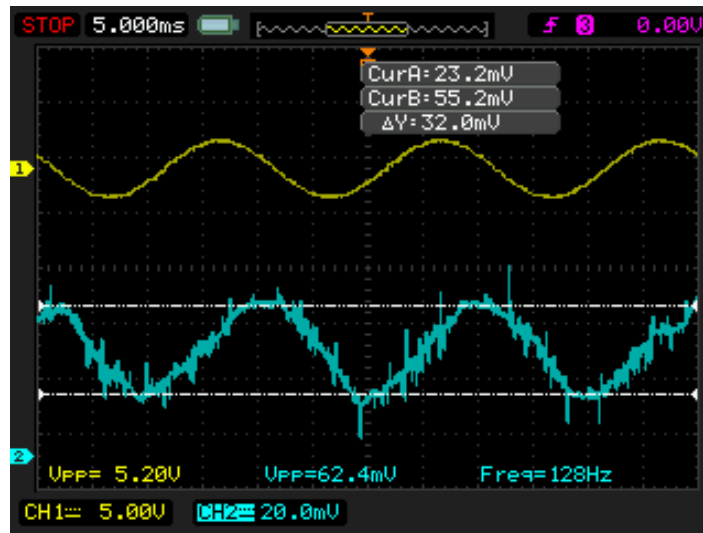


Figure 7-3 – CMRR test result

The standard parameter used when measuring the rejection of the common mode is the CMRR. This parameter describes the relationship between the passband gain of the system and the gain of the common mode. To measure this, both inputs of the system must be short-circuited and connected to a function generator which will create a 5V, 50Hz senoidal wave. The image bellow shows how the apparatus were connected.

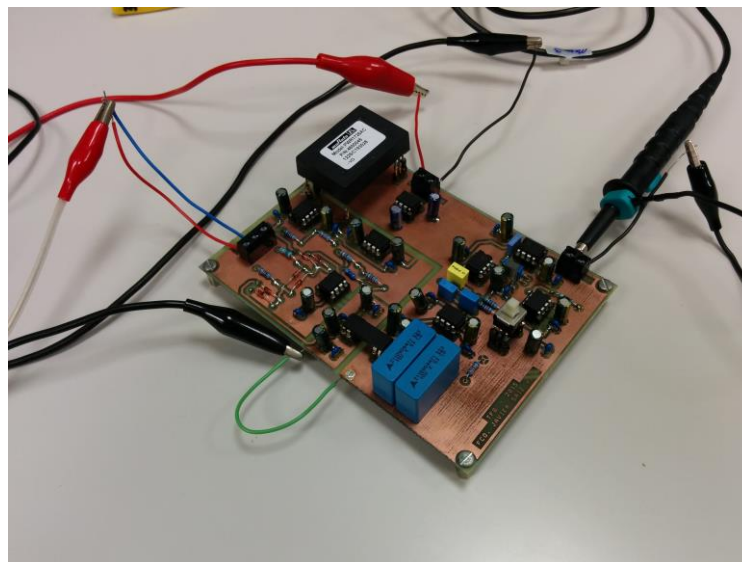


Figure 7-4 – CMRR test setup

The CMRR has the following expression:

$$CMRR = 20 \log \frac{A_D}{A_{MC}} \quad (28)$$

where  $A_D=1120$  is the passband gain and  $A_{MC}$  is the gain of the common mode that is calculated as:

$$A_{MC} = \frac{V_{OUT} (mV)}{V_{IN} (mV)} = \frac{32}{5200} = 0.00615385 \quad (29)$$

and finally the CMRR is:

$$CMRR = 20 \log \frac{A_D}{A_{MC}} = 20 \log \frac{1120}{0.00615385} = 105.2dB \quad (30)$$

Article 51.5.3 of the European-Spanish Legislation UNE-EN 60601-2-47 states that the minimum CMRR, must be 60dB and as our system develops 105.2 dB, it follows the legislation.

### 7.3. Noise Test

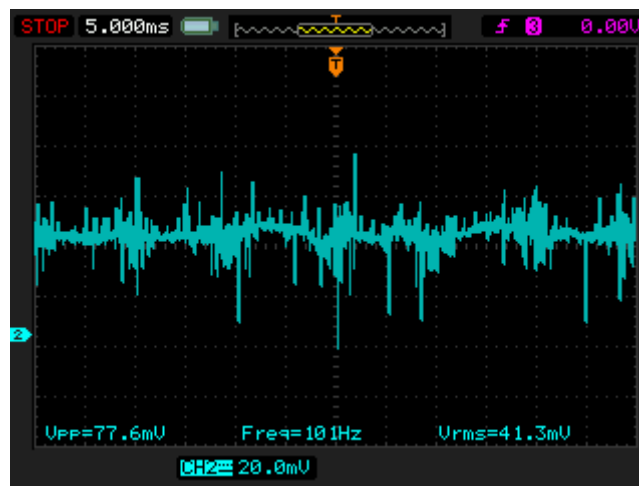


Figure 7-5 – Noise test result

Figure 7-5 shows the amount of internal noise the system has. It is measured short-circuiting both inputs to mass and reading the  $V_{RMS}$  in the output as shown in the following image:

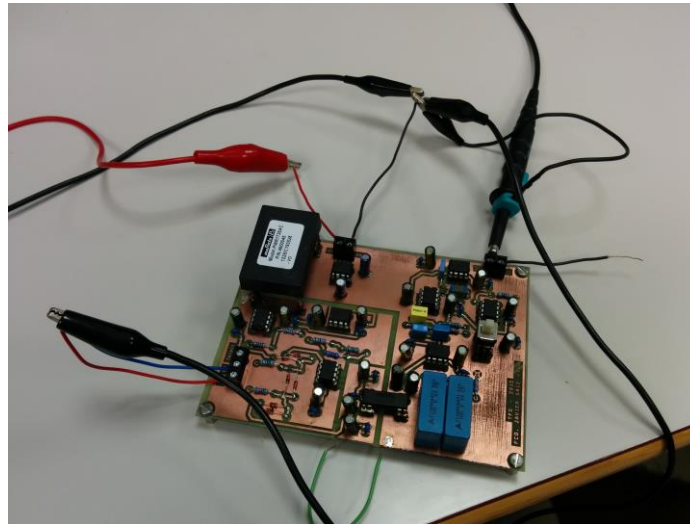


Figure 7-6 – Noise test setup

This test is made to see if the internal noise of the system is small enough not to interfere with the input 1mV signal expected. To do so, we have to calculate the noise RMS referred to the input stage.

$$V_{\text{Noise in the input}} = \frac{V_{\text{Noise in the output}}}{A_D} \quad (31)$$

Being  $A_D$  the passband gain, the noise is:

$$V_{\text{Noise in the input}} = \frac{41.3 \text{ mV}}{1120} = 0.037 \text{ mV} = 37\mu\text{V} \quad (32)$$

#### 7.4. Common Mode Shielded Driver Test

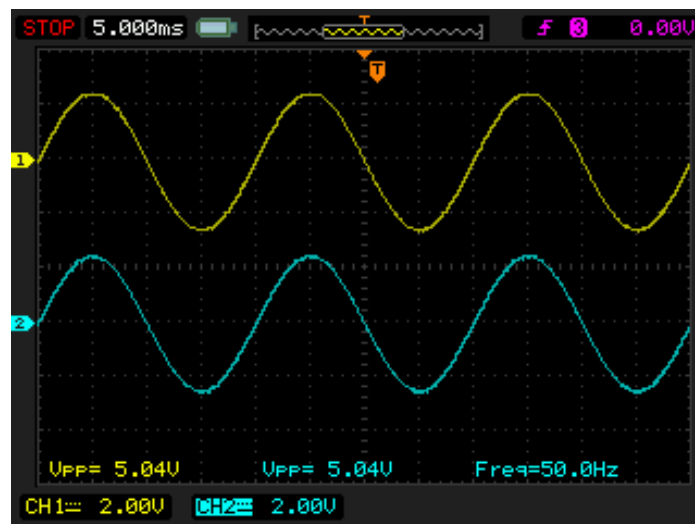


Figure 7-7 – Common Mode Shielded Driver test

An additional test was performed in the follower to record its behaviour inside our system. As expected, the input of the system signal CH1 and output of the follower signal CH2 are the same which shows that the follower had unitary gain. To obtain this test, a signal of 5V and 50Hz was introduced and the connection was the following:

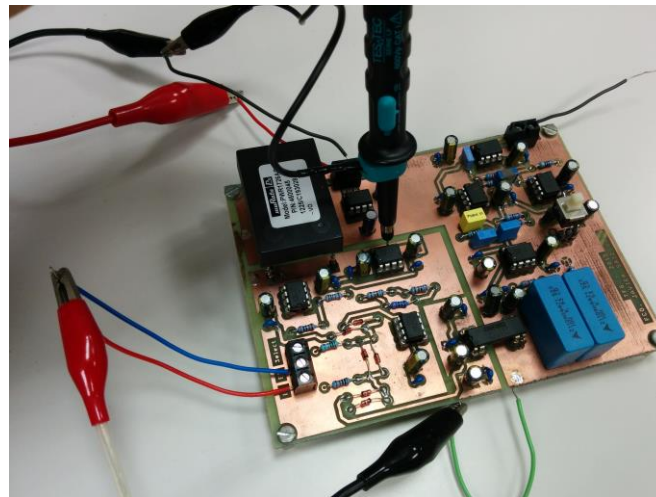


Figure 7-8 – Common Mode Shielded Driver test setup

### 7.5. Driven-Right-Leg circuit

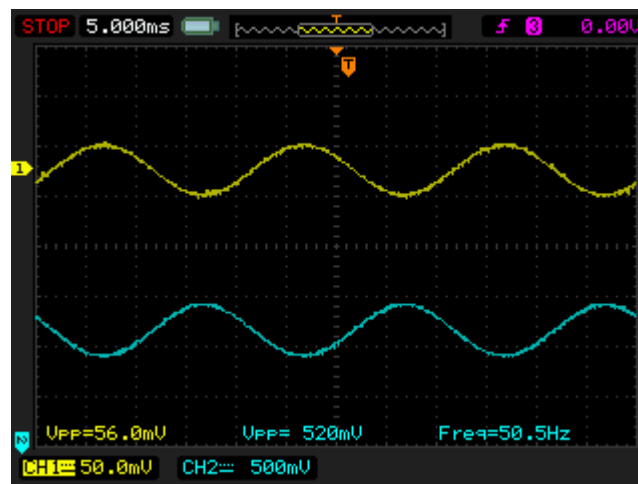


Figure 7-9 – Driven-Right-Leg circuit

The signal given off by the 3<sup>rd</sup> electrode was also a useful measurement to ensure the correct performance of the system. The input to the DRL circuit was CH1 and the output CH2. The gain for which this amplifier was designed was -10. As can be observed in the figure the gain is:

$$G_{GA} = \frac{\text{Output } V_{pp}}{\text{Input } V_{pp}} = \frac{520 \text{ mV}}{56.0 \text{ mV}} = 9.3 \quad (33)$$

Although the gain in the equation which is calculated using the modulus is positive, as the amplifier clearly inverts the signal, the actual gain  $G_{GA}$  is -9.3. This gain follows our designed specifications.

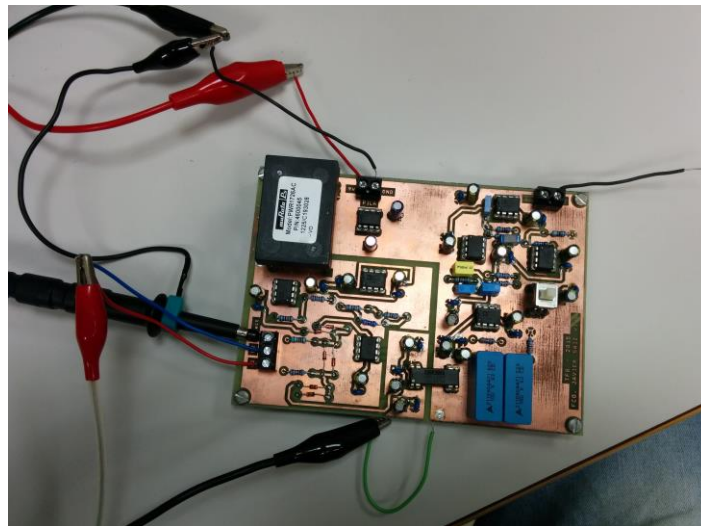


Figure 7-10 – Driven-Right-Leg test setup

## 7.6. Test on Sport Activities

After the preliminary tests were completed it was time to test the system in humans. The aim of this project was to design and operate an ECG system that would be used during sportive activities therefore the trials were conducted while our subject was running in a treadmill.



Figure 7-11 – Test conditions

In order to do so, a special t-shirt with built-in electrodes was used provided by Smart Tech Solutions, Nuubo.



Figure 7-12 – Special t-shirt used in test

Measurements were taken at rest with and without the 50 Hz filter to observe the effect the filter has in the signal, Figure 7-13 and Figure 7-14 respectively.

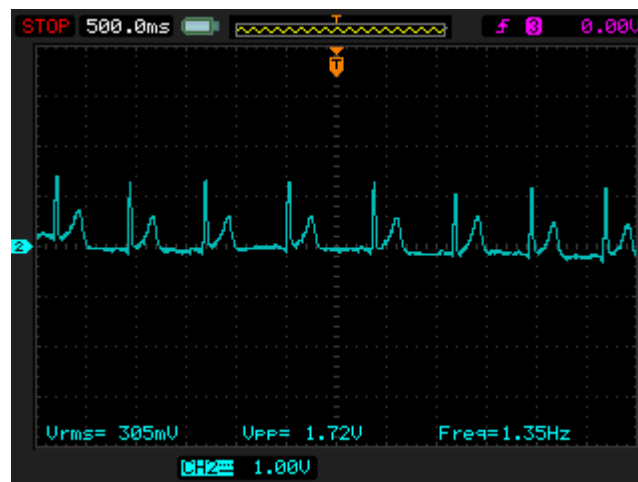


Figure 7-13 – Measurement with the 50 Hz filter



Figure 7-14 – Measurement without the 50 Hz filter

With the 50Hz filter, the QRS complex of the signal had an amplitude of 1.4V more or less and as the period between R peaks was 750ms, the heart rate was approximately 80bpm, hereinafter the basal rate. Without the 50Hz filter, the QRS complex had an amplitude of 2.4V, 70% more than with the filter. The rate undergoes no significant change as in both cases the subject was at rest.

To be seen more clearly, a measurement were in the first half the filter was not operative and in the second half it was is shown in Figure 7-15. Although the second part of the signal is clearer and has less noise, there is also a decrease in the amplitude of the R pulse as comented before and the S wave disappears.



Figure 7-15 – Difference between without and with 50Hz filter



Measurements were then taken while the subject walked at 6 km/h and ran at 8km/h without the filter to observe how the cardiac pulse changed and as can be seen in Figure 7-16 and Figure 7-17, there is very little muscular noise introduced in the signal.



Figure 7-16 – Measurement taken while running at 6km/h

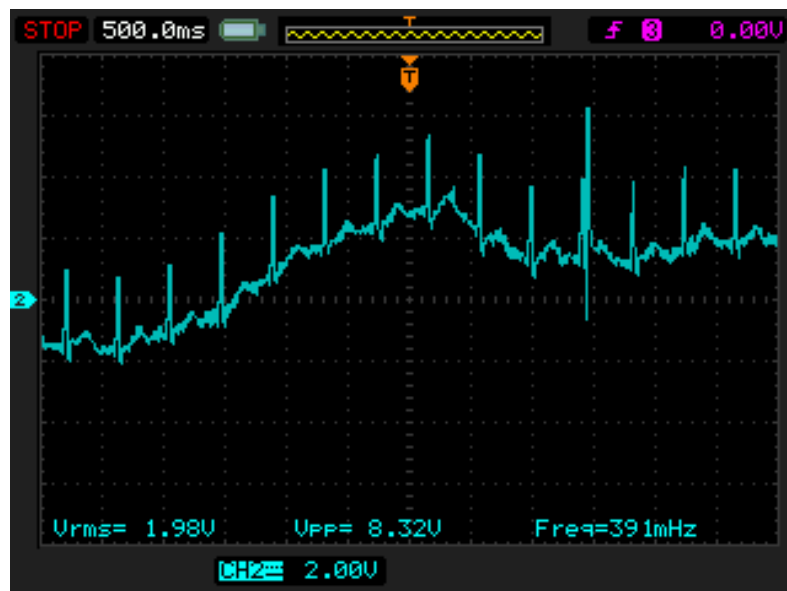


Figure 7-17 – Measurement taken while running at 8km/h

When running at 6km/h, the signal picks up some muscular tremors and the heart rate is 120bpm, which is an increase of 50% from the basal rate. At 8km/h, the signal experiences wandering baseline and there is more muscular noise. The heart rate is faster, more or less 200bpm, which makes sense as the subject had to run faster.

## 8. VISUALISATION AND TREATMENT OF THE SIGNAL

### 8.1. Objectives

The ECG was filtered using analog filters and this part of the project is going to focus in digitalizing the signal using a Data Acquisition USB Device and filtering it using the digital filter tool that LabView (short for Laboratory Virtual Instrument Engineering Workbench) offers.

### 8.2. DAQ USB Device

The acquisition device used was a NI USB-6001 provided by the DIE (Departamento de Ingeniería Electronica) and was used to digitalize the analog signal generated in the circuit board. The characteristics of the DAQ device are included in the Specifications Statement. The DAQ device is shown in the following figure:



Figure 8-1 – National Instruments DAQ Device

### 8.3. LabView Interface

LabView Fall 2012 was used for this part as the UPV has an educational license students can use. LabView enables the user to create virtual instruments, hereinafter VI and using the DAQ device, the signal can be introduced to the program and treated accordingly. LabView creates a Front Panel (shown in Figure 8-2) which is a user interface where the signals will be visualized and the Block Diagram (shown in Figure 8-3) where the graphical programming is done.



Figure 8-2 – User Panel Layout

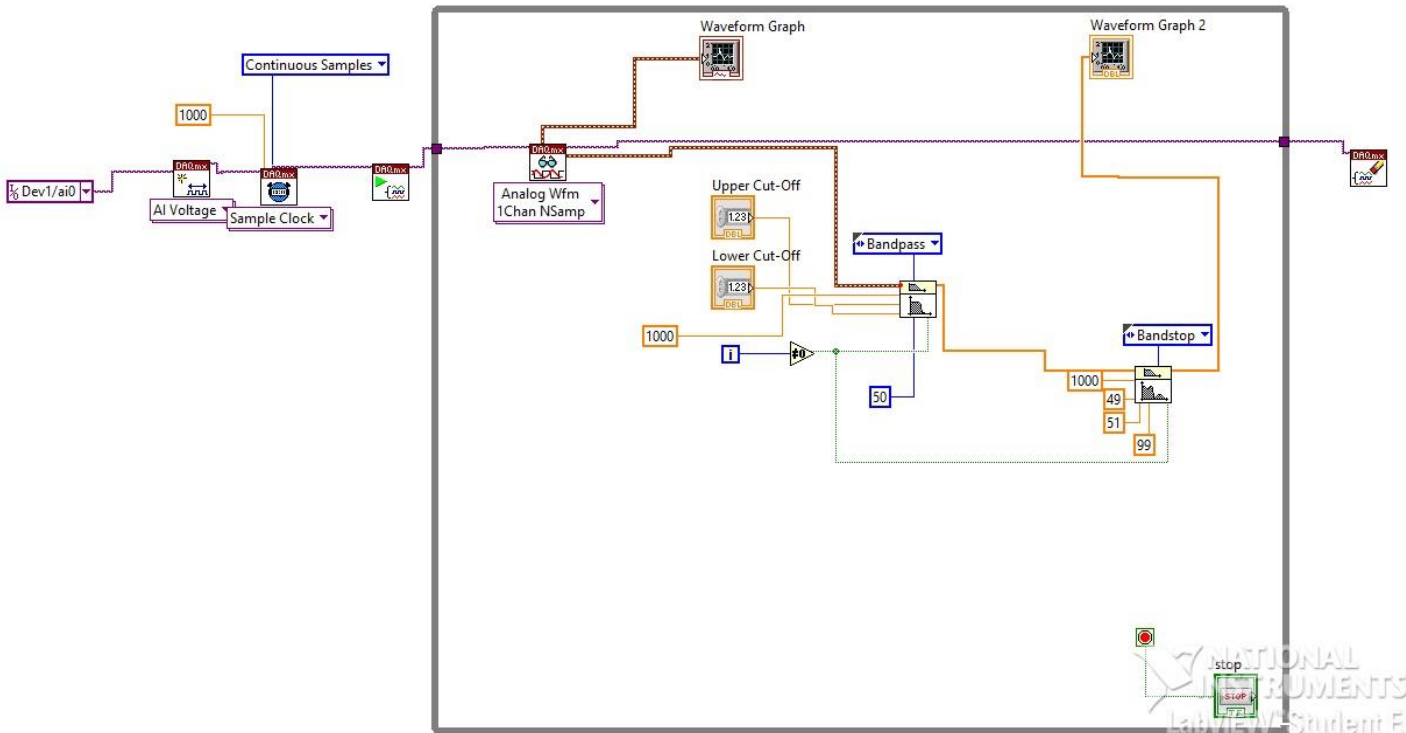


Figure 8-3 – Final Block Diagram

#### 8.4. Code implemented

The Block Diagram was constructed using DAQmx driver software which is used to communicate between the hardware (DAQ device) and the programming language used (LabVIEW). Firstly, in the DAQmx pallet (Figure 8-4) that can be found in the Measurement I/O pallet, the DAQmx Create Virtual Channel block had to be laid down. This function takes the physical channel, Dev01/ai0 in our case which represents the 0 analog input in the device 1, and converts it to a virtual channel.

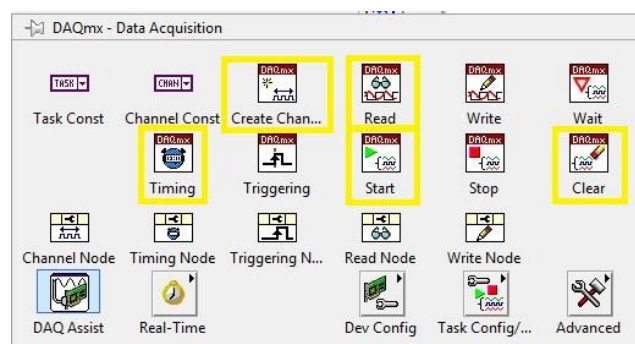


Figure 8-4 – DAQmx Pallet

For the timing parameters, the DAQmx Timing function was used where the number of samples per second (rate) required and the sample mode was configured. The rate chosen was 1000Hz and the sample mode used was continuous samples so continuous data could be streamed into the program. Next, the DAQmx Start Task function was used as it is what actually begins the acquisition. Once the measurements are being taken, the DAQmx Read VI is used to read the data. In the configuration of this function Analog, Single Channel, Multiple Samples, Waveform

was chosen as the objective is to view multiple measurements at a time and view the data in a waveform. As continuous samples are required, this last function is introduced in a Loop which will execute until the User presses the STOP button. Now, as the aim is to view the original signal and the filtered signal at the same time, the path separates and one goes into a Waveform graph function and the other into a series of Filter functions. The first filter function is a 50<sup>th</sup> Order Butterworth Bandpass. Note that once working with digital filters the order of the filter can be far greater than that of an analog filter. The Cutoff Frequencies of the filter can be introduced by the User (as seen in Figure 8-5) as long as the higher cutoff frequency is bigger than the lower. After the Butterworth, an Elliptical Bandstop filter is used to filter the 50Hz frequency interference. This filter has the characteristic of being able to fix the stopband attenuation (dB) as well as the cutoff frequencies, in this case, the attenuation was fixed to 99dB and as the 50Hz frequency component was our target, the higher cutoff frequency was fixed to 51Hz and the lower to 49Hz. The sample frequency in both filters remained 1000Hz. The last thing needed to finish the program and clear the task in order to free up resources is to use the DAQmx Clear Task function outside the loop.

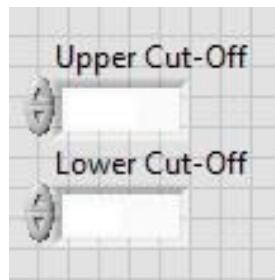


Figure 8-5 – User interface used to specify the Cut-off frequencies required

## 8.5. Results

Knowing that the safety requirements were met, the subject was connected to the board and to the computer via the DAQ Device. The setup for the following test is shown in Figure 8-6.



Figure 8-6– Test Setup

This test was done while the subject was at rest and the results shown in the User Panel are the following.



Figure 8-7 – Results (Input signal taken from Function Generator)

The upper Waveform graph shows the signal as it leaves the board which had the 50Hz filter switched off. The signal has an amplitude of 2V peak-to-peak more or less and a heart rate of 75bpm. The lower Waveform shows the digitally filtrated signal, as can be observed, there is almost no interferences and although the QRS complex is a bit smaller (1.5V peak-to-peak), the signal is much clearer.



## 9. CONCLUSION

Although there were some limitations, all the specifications were met and the objectives of this project were fully fulfilled. There are many things I learned while working on this project. Not only I became comfortable in a lab and got used to working with oscilloscopes and soldering ions but I also got to learn how to use programs such as OrCAD and LabView or how circuit boards were manufactured. The elaboration of this project has also taught me how to search and select the appropriate information effectively and use the legislation that regulates the particular requirements for the basic safety and essential performance of electrocardiographic monitoring equipment. In summary, by doing this project I have:

- Practiced the concepts learned in many subjects throughout the bachelor such as Tecnología Electrónica, Sistemas Electrónicos, Tecnología Automática, Sistemas Automáticos, Teoría de Circuitos and Proyectos.
- Learned how to operate OrCAD as well as LabView
- Learned how to use all the apparatus involved in the creation and testing of the board
- Learned how to write a technical review, search for useful information and refer this information properly
- Learned about the legislation and the differences between the UNE and the ANSI



## 10. LIST OF FIGURES

Figure 2-1 – Heart’s physiology [1].....	10
Figure 2-2 – Myocardium muscles [2] .....	11
Figure 2-3 – Complete heart cycle [3] .....	11
Figure 2-4 – Action potential development.....	12
Figure 2-5 – Ionic exchange present in action potential [4] .....	13
Figure 2-6 – Relationship between action potentials and the ECG [5] .....	14
Figure 2-7 – W.Einthoven’s first ECG system [6] .....	14
Figure 2-8 – Standard Leads [7].....	15
Figure 2-9 – ECG depending on the lead used [8] .....	15
Figure 2-10 – Typical ECG waveform [9].....	16
Figure 2-11 – Normal chest leads. Modified from [10].....	17
Figure 4-1 – ECG Typical Peak-to-Peak Value. Modified from [9].....	18
Figure 4-2 – Typical ECG frequency spectrum [8].....	19
Figure 4-3 – Effect of the main grid in the patient’s body [8].....	20
Figure 4-4 – (a) Leads in a loop with a magnetic field going through it. ....	20
Figure 4-5 – Muscle tremor in ECG [11] .....	21
Figure 4-6 – Wandering baseline in ECG [11] .....	21
Figure 4-7 – Electrode model .....	22
Figure 4-8 – Variation of skin impedance with frequency [12].....	23
Figure 4-9 – Effect of electrolyte paste in reducing the epidermis’ impedance .....	24
Figure 5-1 – Block Diagram.....	25
Figure 5-2 – Capacitor Barrier .....	26
Figure 5-3 – Input Stage .....	26
Figure 5-4 – Isolation Stage .....	29
Figure 5-5 – High pass filter.....	30
Figure 5-6 – Typical High Pass Filter frequency response. Modified from [14].....	31
Figure 5-7 - Amplifier .....	31
Figure 5-8 – Low Pass Filter .....	32
Figure 5-9 – Typical Low Pass Filter frequency response. Modified from [14] .....	33
Figure 5-10 – Notch Filter .....	33
Figure 5-11 – Typical Notch Filter frequency response [14] .....	35
Figure 5-12 – Switch schematic.....	35
Figure 5-13 – Switch Inner diagram and connections. ....	35
Figure 5-14 – Common Mode Shield Driver .....	36
Figure 5-15 – Zoom in section of the Layout (see 5.1) where the shielding is coloured green.....	36
Figure 5-16 – Driven Right Leg .....	37
Figure 5-17 – Isolated Power Supply .....	38
Figure 5-18 – Isolated power supply block diagram .....	38
Figure 6-1 – OrCAD Capture interface.....	39
Figure 6-2 - Libraries.....	40
Figure 6-3 – OrCAD Layout interface .....	40
Figure 6-4 – Library Manager .....	41
Figure 6-5 – Top transparency.....	42
Figure 6-6 – Bottom transparency.....	42
Figure 6-7 – Both transparencies combined.....	43
Figure 6-8 – UV light exposition process .....	43



Figure 6-9 – Photographic processing .....	44
Figure 6-10 – Chemical Attack.....	44
Figure 6-11 – Board after chemical bath .....	44
Figure 6-12 – Board rinsed .....	44
Figure 6-13 – Board with drill .....	45
Figure 6-14 – Board being drilled .....	45
Figure 6-15 – Board with the holes drilled .....	45
Figure 6-16 – Finished Circuit Board.....	46
Figure 7-1 – Frequency response without the 50Hz Filter.....	47
Figure 7-2 – Frequency response with the 50Hz Filter .....	48
Figure 7-3 – CMRR test result.....	49
Figure 7-4 – CMRR test setup .....	49
Figure 7-5 – Noise test result .....	50
Figure 7-6 – Noise test setup.....	51
Figure 7-7 – Common Mode Shielded Driver test .....	51
Figure 7-8 – Common Mode Shielded Driver test setup .....	52
Figure 7-9 – Driven-Right-Leg circuit .....	52
Figure 7-10 – Driven-Right-Leg test setup .....	53
Figure 7-11 – Test conditions .....	53
Figure 7-12 – Special t-shirt used in test .....	54
Figure 7-13 – Measurement with the 50 Hz filter .....	54
Figure 7-14 – Measurement without the 50 Hz filter .....	54
Figure 7-15 – Difference between without and with 50Hz filter .....	55
Figure 7-16 – Measurement taken while running at 6km/h.....	56
Figure 7-17 – Measurement taken while running at 8km/h.....	56
Figure 8-1 – National Instruments DAQ Device .....	57
Figure 8-2 – User Panel Layout.....	57
Figure 8-3 – Final Block Diagram .....	58
Figure 8-4 – DAQmx Pallet .....	58
Figure 8-5 – User interface used to specify the Cut-off frequencies required.....	59
Figure 8-6– Test Setup.....	59
Figure 8-7 – Results (Input signal taken from Function Generator) .....	60





## 11. REFERENCES

- [1] [https://commons.wikimedia.org/wiki/File:Diagram\\_of\\_the\\_human\\_heart.svg](https://commons.wikimedia.org/wiki/File:Diagram_of_the_human_heart.svg)
- [2] <http://www.ubooks.pub/Books/ON/B0/E28R8369/P4C2S2U27.html>
- [3] [https://upload.wikimedia.org/wikipedia/commons/3/38/2027\\_Phases\\_of\\_the\\_Cardiac\\_Cycle.jpg](https://upload.wikimedia.org/wikipedia/commons/3/38/2027_Phases_of_the_Cardiac_Cycle.jpg)
- [4] <http://galleryhip.com/ion-movements-at-resting-potential.html>
- [5] <http://www.profesorenlinea.cl/Ciencias/Electrocardiograma.html>
- [6] <http://www.historiadelamedicina.org/einthoven.html>
- [7] <http://www.medicine.mcgill.ca/physio/vlab/cardio/setup.htm>
- [8] Bioelectronica Señales Bioelectronicas José M. Ferrero Corral Ed. UPV
- [9] <https://en.wikipedia.org/wiki/Electrocardiography>
- [10] <https://quizlet.com/10648451/flashcards-flash-cards/>
- [11] [http://www.mauvila.com/ECG/ecg\\_artifact.htm](http://www.mauvila.com/ECG/ecg_artifact.htm)
- [12] Biomedical Engineering, IEEE Transactions on; Javier Rosell, Josep Colominas, Pere Riu, Ramon Pallas-Areny, John G Webster
- [13] <http://urgenciasudd.blogspot.com.es/2014/06/recomendaciones-de-la-aha-2010-sobre.html>
- [14] <http://srtv-2011-2012.wikispaces.com/2.1.1+Tipos+de+filtros>



# Layouts

Author: Francisco Javier Saiz Vivó

Tutor: Francisco Javier Saiz Rodriguez

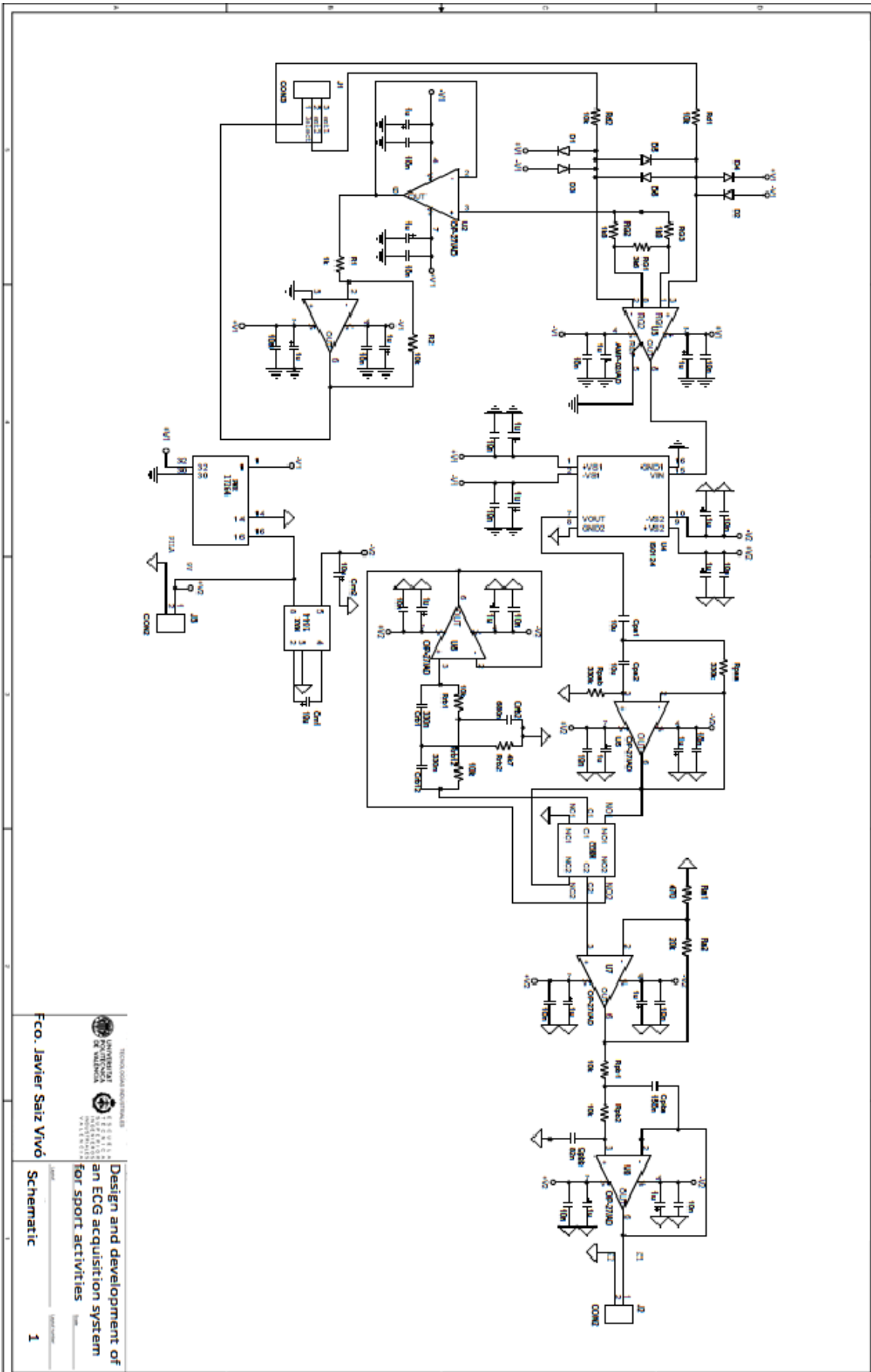




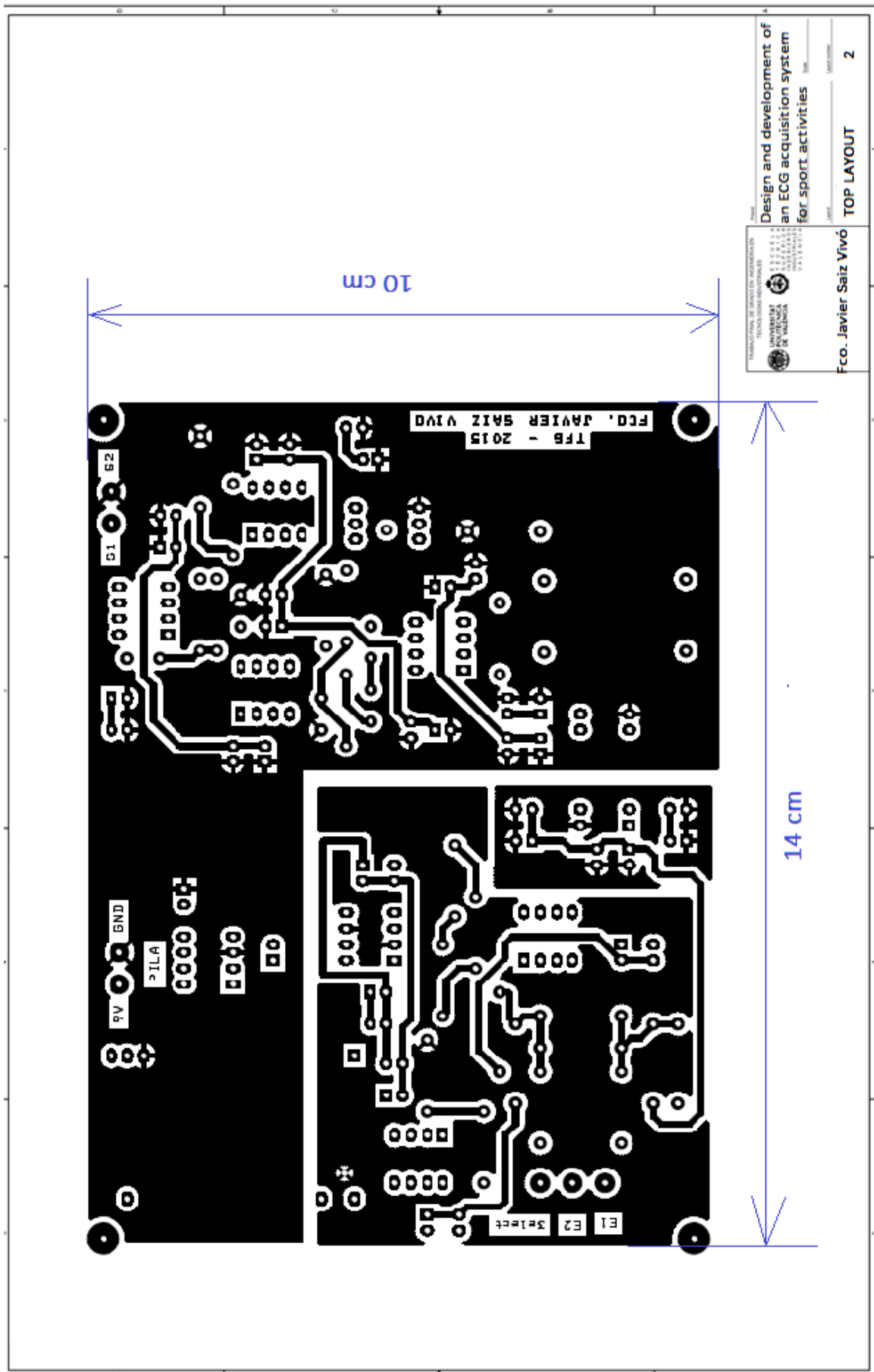
## INDEX

1. Layout 1:Schematic layout .....	69
2. Layout 2: Top layout .....	70
3. Layout 3: Bottom layout .....	71
4. Layout 4: Components layout .....	72



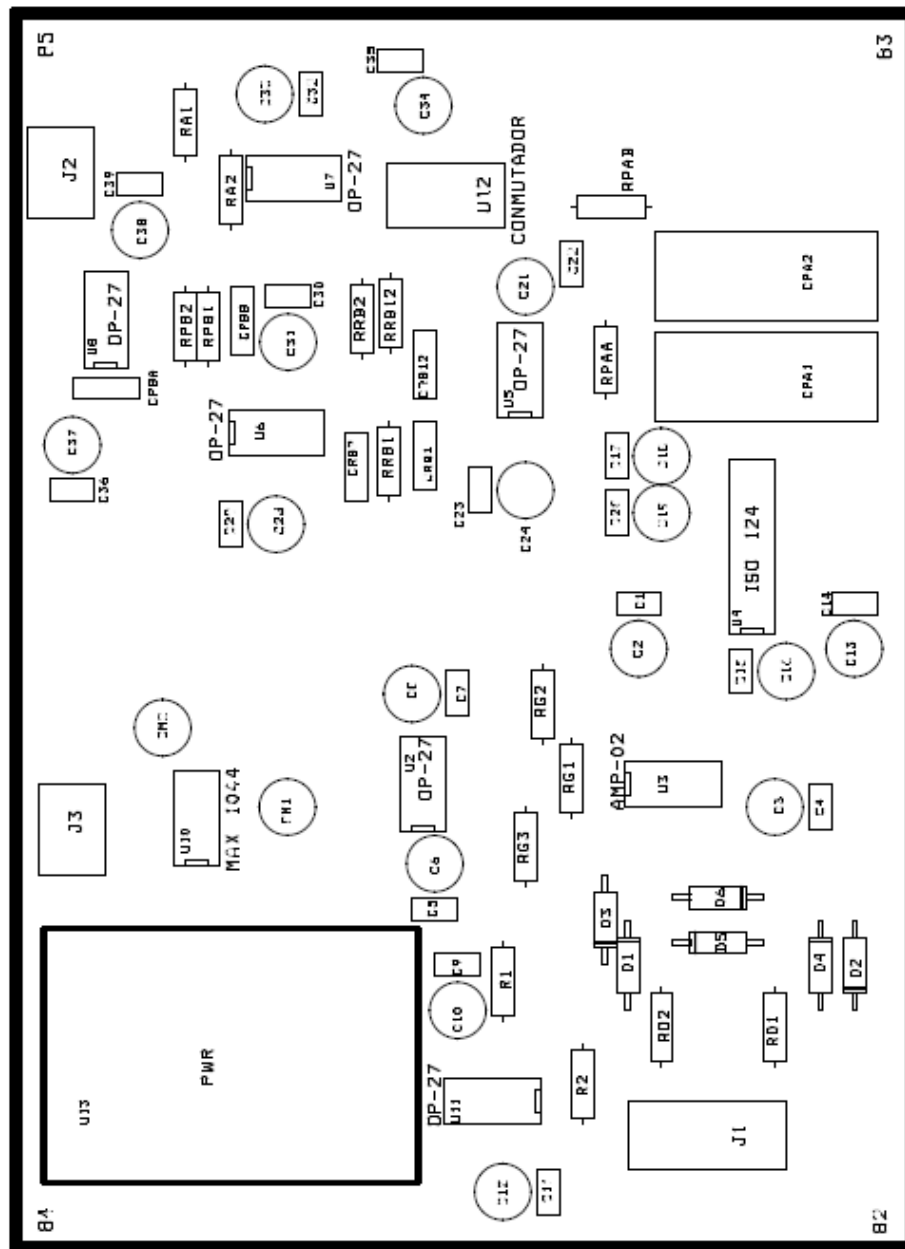


	<p>UNIVERSITAT DE VALÈNCIA</p> <p>ESCUELA TÉCNICA SUPERIOR DE INGENIEROS INDUSTRIALES VALENCIA</p>
<p>Fco. Javier Saliz Vivó</p>	<p>Design and development of an ECG acquisition system for sport activities</p>
<p>Schematic</p>	<p>1</p>











# BUDGET

Author: Francisco Javier Saiz Vivó

Tutor: Francisco Javier Saiz Rodriguez





## INDEX

1. Budget for 1 Circuit Board.....	77
2. Budget for 100 Circuit Boards.....	79
3. Budget for Visualization System.....	80





# BUDGET

For 1 Circuit Board

Quantity	Units	Description	Unitary Price (€)	Discount	Row Total (€)
6		OP-27	2.89		17.340
1		MAXIM1044	2.74		2.740
1		PWR1726	40.17		40.170
1		AMP-02	11.39		11.390
1		ISO124	17.11		17.110
1		Commutator ESB33	1.67		1.670
6		Diodes (1N4148)	0.087		0.522
16		Resistances (0.25W, 1%)	0.489		7.824
23		Capacitors	0.276		6.348
2		Capacitors (10 $\mu$ F)	2.21		4.420
20		Polarized Capacitors	0.48		9.600
8		Plug-in socket	1.08		8.640
1		Pin line (20 pins)	0.238		0.238
2		Connector (2 Connexions)	0.07		0.140
1		Connector (3 Connexions)	0.1		0.100



1		9V Battery	4.16	4.160
1		Battery holder	0.38	0.380
1		Board	10.43	10.430
150	(h)	Design by Industrial Engineer (social security included)	20	3000
3	(h)	Manufacturing by Industrial Engineer (social security included)	15	45

<b>Subtotal</b>	3188.042 €
<b>IVA (21%)</b>	669.489 €
<b>Total</b>	<b>3857.531 €</b>
<b>Cost/Board</b>	<b>3857.531 €</b>



# BUDGET

For 100 Circuit Boards

Quantity	Description	Unitary Price (€)	Row Total (€)
1	Subtotal 1 Circuit Board	3188.042	3188.042
99	Subtotal-Design Costs	188.042	18616.158
	<b>Subtotal</b>		21804.200 €
	<b>IVA (21%)</b>		4578.882 €
	<b>Total</b>		26383.082 €
	<b>Cost/Board</b>		263.830 €





# BUDGET

For Visualization System

Quantity	Units	Description	Unitary Price (€)	Discount	Row Total (€)
1		Computer with Windows 7, Core i3	300		300.000
1		DAQ DEVICE NI USB-6001	199		199.000
3		Profesional Cables	3.33		10.000
3		Conductive Adhesive Hydrogel Electrodes	0.4		1.200
1		LabView Educational License	0		0
20	(h)	Design by Industrial Engineer (social security included)	20		400
<b>Subtotal</b>					910.200 €
<b>IVA (21%)</b>					191.142 €
<b>Total</b>					1101.342 €



UNIVERSITAT  
POLITÈCNICA  
DE VALÈNCIA



# STATEMENT OF SPECIFICATIONS

Author: Francisco Javier Saiz Vivó

Tutor: Francisco Javier Saiz Rodriguez





## INDEX

1. Component List.....	83
2. Component Specifications and Legislation.....	83
3. CD Contents.....	96





## 1. COMPONENT LIST

Component	Number
AMP02	1
PWR-17264	1
MAX 1044	1
ISO 124	1
OP27	6
DIODES 0.5W	6
CONMUTATOR	1
3 CONEXION CONNECTOR	1
2 CONEXION CONNECTOR	1
9V Battery	1
Battery Holder	1
<b>RESISTENCES:</b>	
470	1
1k	1
1k8	2
3k6	1
4k7	1
10k	7
20k	1
330k	2
<b>CAPACITORS:</b>	
10n	18
82n	1
150n	1
330n	2
680n	1
10 micros	2
<b>POLARIZED CAPACITORS:</b>	
1micro	18
10micro	2

## 2. COMPONENT SPECIFICATIONS AND LEGISLATION

In order not to make this project too long, the specifications of all the components can be found in the CD attached to this report. The following pages show the first page of these specifications and also the legislations consulted

### FEATURES

- Low noise: 80 nV p-p (0.1 Hz to 10 Hz), 3 nV/√Hz
- Low drift: 0.2 μV/°C
- High speed: 2.8 V/μs slow rate, 8 MHz gain bandwidth
- Low  $V_{os}$ : 10 μV
- Excellent CMRR: 126 dB at VCM of ±11 V
- High open-loop gain: 1.8 million
- Fits OP07, 5534A sockets
- Available in die form

### GENERAL DESCRIPTION

The OP27 precision operational amplifier combines the low offset and drift of the OP07 with both high speed and low noise. Offsets down to 25 μV and maximum drift of 0.6 μV/°C make the OP27 ideal for precision instrumentation applications. Exceptionally low noise,  $e_n = 3.5$  nV/√Hz, at 10 Hz, a low 1/f noise corner frequency of 2.7 Hz, and high gain (1.8 million), allow accurate high-gain amplification of low-level signals. A gain-bandwidth product of 8 MHz and a 2.8 V/μs slew rate provide excellent dynamic accuracy in high speed, data-acquisition systems.

A low input bias current of ±10 nA is achieved by use of a bias current cancellation circuit. Over the military temperature range, this circuit typically holds  $I_B$  and  $I_{os}$  to ±20 nA and 15 nA, respectively.

The output stage has good load driving capability. A guaranteed swing of ±10 V into 600 Ω and low output distortion make the OP27 an excellent choice for professional audio applications.

(Continued on Page 3)

### PIN CONFIGURATIONS

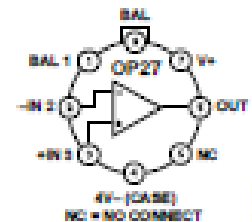


Figure 1. 8-Lead TO-99 (J-Suffix)

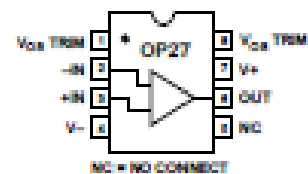


Figure 2. 8-Lead CERDIP - Glass Hermetic Seal (Z-Suffix), 8-Lead PDIP (P-Suffix), 8-Lead SO (S-Suffix)

### FUNCTIONAL BLOCK DIAGRAM

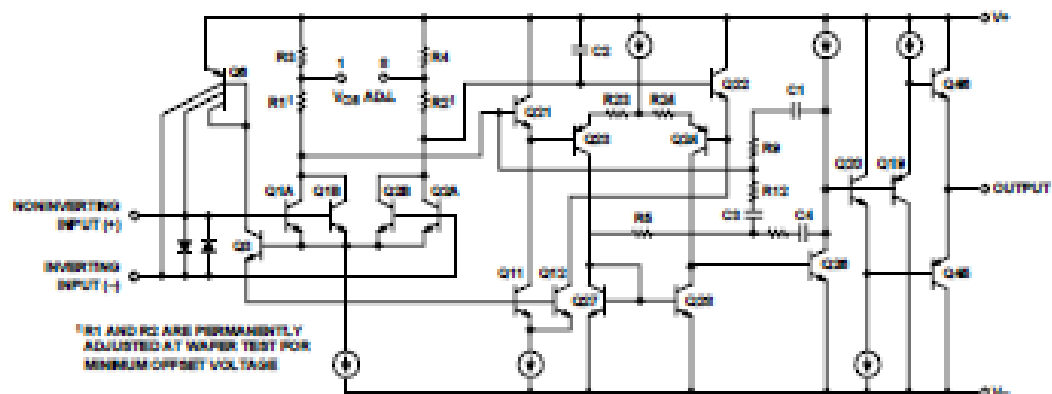


Figure 3.

Rev. F

Information furnished by Analog Devices is believed to be accurate and reliable. However, no responsibility is assumed by Analog Devices for its use, nor for any infringement of patents or other rights of third parties that may result from its use. Specifications subject to change without notice. No license is granted by implication or otherwise under any patent or patent rights of Analog Devices. Trademarks and registered trademarks are the property of their respective owners.

One Technology Way, P.O. Box 9106, Norwood, MA 02062-9106, U.S.A.  
Tel: 781.328.4700 [www.analog.com](http://www.analog.com)  
Fax: 781.461.5113 ©2006 Analog Devices, Inc. All rights reserved.



# High Accuracy Instrumentation Amplifier

## AMP02

### FEATURES

- Low Offset Voltage: 100  $\mu$ V max
- Low Drift: 2  $\mu$ V/ $^{\circ}$ C max
- Wide Gain Range: 1 to 10,000
- High Common-Mode Rejection: 115 dB min
- High Bandwidth (G = 1000): 200 kHz typ
- Gain Equation Accuracy: 0.5% max
- Single Resistor Gain Set
- Input Overvoltage Protection
- Low Cost
- Available in Die Form

### APPLICATIONS

- Differential Amplifier
- Strain Gage Amplifier
- Thermocouple Amplifier
- RTD Amplifier
- Programmable Gain Instrumentation Amplifier
- Medical Instrumentation
- Data Acquisition Systems

### FUNCTIONAL BLOCK DIAGRAM

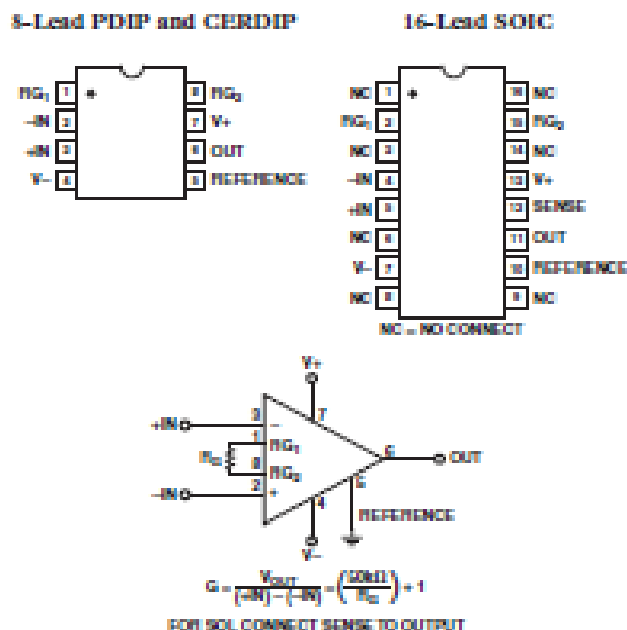


Figure 1. Basic Circuit Connections

### GENERAL DESCRIPTION

The AMP02 is the first precision instrumentation amplifier available in an 8-lead package. Gain of the AMP02 is set by a single external resistor and can range from 1 to 10,000. No gain set resistor is required for unity gain. The AMP02 includes an input protection network that allows the inputs to be taken 60 V beyond either supply rail without damaging the device.

Laser trimming reduces the input offset voltage to under 100  $\mu$ V. Output offset voltage is below 4 mV, and gain accuracy is better than 0.5% for a gain of 1000. ADI's proprietary thin-film resistor process keeps the gain temperature coefficient under 50 ppm/ $^{\circ}$ C.

Due to the AMP02's design, its bandwidth remains very high over a wide range of gain. Slew rate is over 4 V/ $\mu$ s, making the AMP02 ideal for fast data acquisition systems.

A reference pin is provided to allow the output to be referenced to an external dc level. This pin may be used for offset correction or level shifting as required. In the 8-lead package, sense is internally connected to the output.

For an instrumentation amplifier with the highest precision, consult the AMP01 data sheet.

### REV. E

Information furnished by Analog Devices is believed to be accurate and reliable. However, no responsibility is assumed by Analog Devices for its use, nor for any infringements of patents or other rights of third parties that may result from its use. No license is granted by implication or otherwise under any patent or patent rights of Analog Devices. Trademarks and registered trademarks are the property of their respective companies.

One Technology Way, P.O. Box 9106, Norwood, MA 02062-9106, U.S.A.  
Tel: 781/329-4700 [www.analog.com](http://www.analog.com)  
Fax: 781/326-8703 © Analog Devices, Inc., 2002. All rights reserved.





### FEATURES

- 8000V Isolation Test Voltage
- No External Parts Required
- Remote On/Off
- Low-Barrier Capacitance
- RoHS Compliant
- Synchronizable

### APPLICATIONS

- Biomedical Data Acquisition
- Industrial Process Equipment
- Data Acquisition
- Test Equipment
- Portable Equipment

### DESCRIPTION

The PWR1726AC is a single-channel, bipolar output DC/DC/ converter designed for those applications where high-isolation voltage and low-barrier capacitance are critical for system reliability and integrity.

Calculated mean-time-to-failure (MTTF) is in excess of 100 years at an ambient temperature of +25°C and at rated output power. The performance of the PWR1726AC is not derated over its entire specified temperature range of -25°C to +85°C.

Synchronization of the PWR1726AC may be accomplished simply by connecting the Sync-In pin of one unit to the Sync-In pin of another unit. Up to 8 converters may be synchronized in this manner.

The PWR1726AC provides a plus and minus output voltage that is approximately equal to the magnitude of the input voltage. The unit operates over an input voltage range of 7VDC to 16VDC.

Each PWR1726AC isolation barrier is tested per the method set forth by UL544, VDE750, and CSA C22.2.





# MAX1044/ICL7660

## Switched-Capacitor Voltage Converters

### General Description

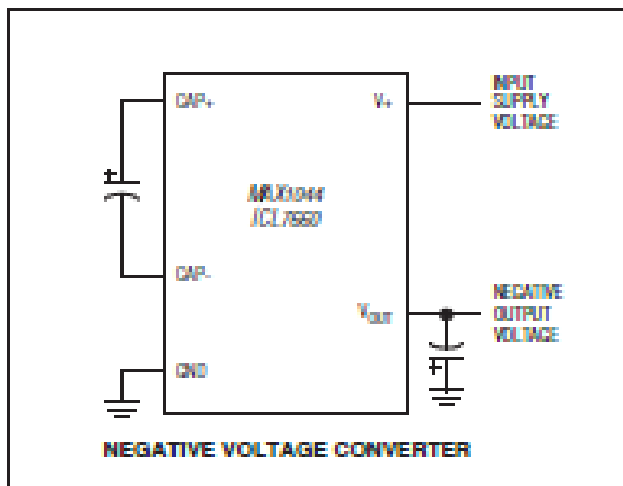
The MAX1044 and ICL7660 are monolithic, CMOS switched-capacitor voltage converters that invert, double, divide, or multiply a positive input voltage. They are pin compatible with the industry-standard ICL7660 and LTC1044. Operation is guaranteed from 1.5V to 10V with no external diode over the full temperature range. They deliver 10mA with a 0.5V output drop. The MAX1044 has a BOOST pin that raises the oscillator frequency above the audio band and reduces external capacitor size requirements.

The MAX1044/ICL7660 combine low quiescent current and high efficiency. Oscillator control circuitry and four power MOSFET switches are included on-chip. Applications include generating a -5V supply from a +5V logic supply to power analog circuitry. For applications requiring more power, the MAX880 delivers up to 100mA with a voltage drop of less than 0.65V.

### Applications

- 5V Supply from +5V Logic Supply
- Personal Communications Equipment
- Portable Telephones
- Op-Amp Power Supplies
- EIA/TIA-232E and EIA/TIA-562 Power Supplies
- Data-Acquisition Systems
- Hand-Held Instruments
- Panel Meters

### Typical Operating Circuit



### Features

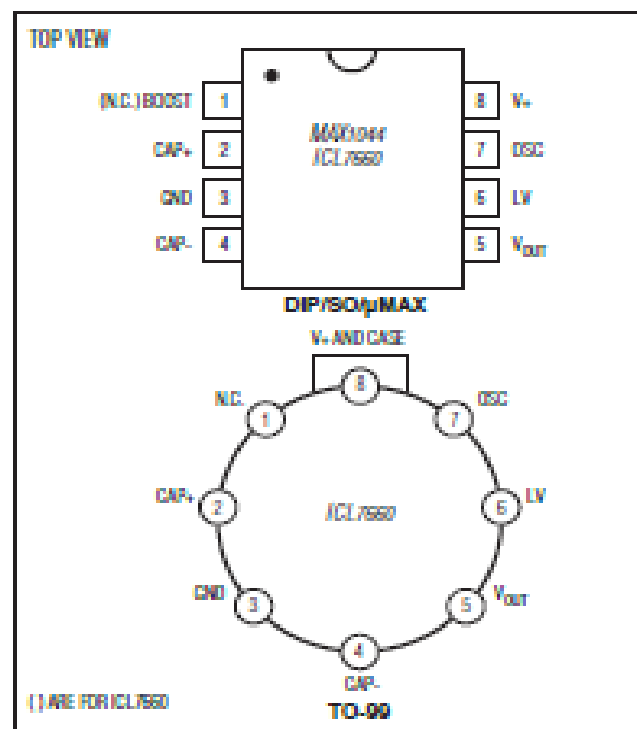
- + Miniature  $\mu$ MAX Package
- + 1.5V to 10.0V Operating Supply Voltage Range
- + 98% Typical Power-Conversion Efficiency
- + Invert, Double, Divide, or Multiply Input Voltages
- + BOOST Pin Increases Switching Frequencies (MAX1044)
- + No-Load Supply Current: 200 $\mu$ A Max at 5V
- + No External Diode Required for Higher-Voltage Operation

### Ordering Information

PART	TEMP. RANGE	PIN-PACKAGE
MAX1044CPA	0°C to +70°C	8 Plastic DIP
MAX1044CSA	0°C to +70°C	8 SO
MAX1044C/D	0°C to +70°C	Diced*
MAX1044EPA	-40°C to +85°C	8 Plastic DIP

Ordering information continued at end of data sheet.  
\* Contact factory for dice specifications.

### Pin Configurations



For pricing, delivery, and ordering information, please contact Maxim Direct at 1-888-629-4642, or visit Maxim's website at [www.maximintegrated.com](http://www.maximintegrated.com).

13-0007; Rev 1; 7/04



- Product Folder
- Sample & Buy
- Technical Documents
- Tools & Software
- Support & Community



## ISO124 Precision Lowest-Cost Isolation Amplifier

### 1 Features

- 100% Tested for High-Voltage Breakdown
- Rated 1500 Vrms
- High IMR: 140 dB at 60 Hz
- 0.010% Maximum Nonlinearity
- Bipolar Operation:  $V_{IO} = \pm 10$  V
- DIP-16 and SO-28
- Ease of Use: Fixed Unity Gain Configuration
- $\pm 4.5$ -V to  $\pm 18$ -V Supply Range

### 2 Applications

- Industrial Process Control:
  - Transducer Isolator, Isolator for Thermocouples, RTDs, Pressure Bridges, and Flow Meters, 4-mA to 20-mA Loop Isolation
- Ground Loop Elimination
- Motor and SCR Control
- Power Monitoring
- PC-Based Data Acquisition
- Test Equipment

### 3 Description

The ISO124 is a precision isolation amplifier incorporating a novel duty cycle modulation-demodulation technique. The signal is transmitted digitally across a 2-pF differential capacitive barrier. With digital modulation, the barrier characteristics do not affect signal integrity, thus resulting in excellent reliability and good high-frequency transient immunity across the barrier. Both barrier capacitors are imbedded in the plastic body of the package.

The ISO124 is easy to use. No external components are required for operation. The key specifications are 0.010% maximum nonlinearity, 50-kHz signal bandwidth, and 200- $\mu$ V/ $^{\circ}$ C  $V_{OS}$  drift. A power supply range of  $\pm 4.5$  V to  $\pm 18$  V and quiescent currents of  $\pm 5$  mA on  $V_{S1}$  and  $\pm 5.5$  mA on  $V_{S2}$  make the ISO124 ideal for a wide range of applications.

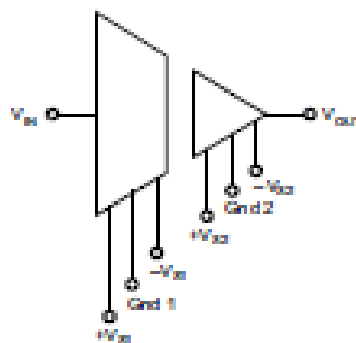
The ISO124 is available in PDIP-16 and SOIC-28 plastic surface-mount packages.

#### Device Information<sup>(1)</sup>

PART NUMBER	PACKAGE	BODY SIZE (NOM)
ISO124	PDIP (16)	17.90 mm $\times$ 7.50 mm
	SOIC (28)	20.01 mm $\times$ 6.61 mm

(1) For all available packages, see the orderable addendum at the end of the data sheet.

### 4 Simplified Schematic



An IMPORTANT NOTICE at the end of this data sheet addresses availability, warranty, changes, use in safety-critical applications, intellectual property matters and other important disclaimers. PRODUCTION DATA.

# Panasonic

## Push Switches/ESB33

### ESB33 Vertical Push Switches

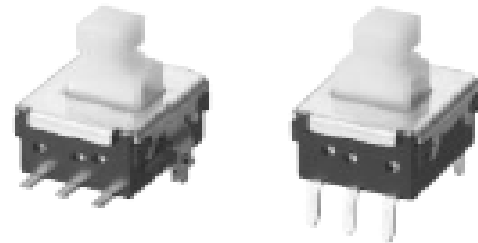
Type: **ESB33 (H=6.0 mm)**

#### ■ Features

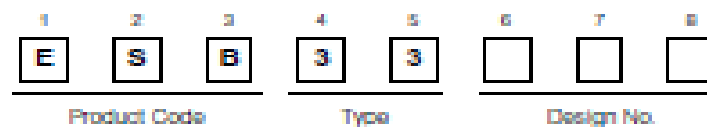
- Low profile (H=6.0 mm)
- 3 N and 5 N operating force availables

#### ■ Recommended Applications

- Operation switches for automobiles (heater control switches etc.)
- Secondary power switches for lower voltage in consumer electronic equipment and different types of mode switches



#### ■ Explanation of Part Numbers



#### ■ Specifications

Rating	50 $\mu$ A 3 Vdc to 0.2 A 14 Vdc (Resistive load)
Travel	Lock travel=1.5 mm Full travel=2.9 mm
Mounting Height	6.0 mm
Poles and Throws	2-poles 2-throws
Operating Mode	Self-lock, Non-lock
Switching Mode	Non-shorting
Minimum Quantity/Packing Unit	100 pcs. Polyethylene Bag (Bulk) / 300 pcs. Embossed Taping (Reel Pack)
Quantity/Carion	2000 pcs. Polyethylene Bag (Bulk) / 1800 pcs. Embossed Taping (Reel Pack)

#### ■ Standard Products

Operating Mode	Terminals	Packaging	Operating Force	Part Numbers	Lever Color
PP	Wave Soldering	Polyethylene Bag (Bulk)	3.0 N±1.0 N	ESB33133	Light Yellow
NL				ESB33134	
PP	Surface Mount	Embossed Taping (Reel )	3.0 N±1.0 N	ESB33535	Light Yellow
NL				ESB33536	

Note: PP=Self-lock NL=Non-lock

Design and specifications are each subject to change without notice. Ask factory for the current technical specifications before purchase and/or use. Should a safety concern arise regarding this product, please be sure to contact us immediately.

00 Oct. 2012



**DISCRETE SEMICONDUCTORS**

# DATA SHEET



## **1N4148; 1N4448** High-speed diodes

Product data sheet  
Supersedes data of 2002 Jan 23

2004 Aug 10





## SPECIFICATIONS

# NI USB-6001

## Low-Cost DAQ USB Device

The following specifications are typical at 25 °C, unless otherwise noted. For more information about the NI USB-6001, refer to the *NI USB-6001/6002/6003 User Guide* available at [ni.com/manuals](http://ni.com/manuals).

## Analog Input

---

### Number of channels

Differential.....4

Single-ended.....8

ADC resolution.....14-bit

Maximum sample rate (aggregate).....20 kS/s

Converter type.....Successive approximation

AI FIFO.....2,047 samples

Trigger sources.....Software, PFI 0, PFI 1



# norma española

UNE-EN 60601-2-47

Junio 2002

<b>TÍTULO</b>	<p><b>Equipos electromédicos</b></p> <p><b>Parte 2-47: Requisitos particulares para la seguridad, incluyendo las características de funcionamiento esencial, de los sistemas de electrocardiografía ambulatoria</b></p> <p><i>Medical electrical equipment. Part 2-47: Particular requirements for the safety, including essential performance, of ambulatory electrocardiographic systems.</i></p> <p><i>Appareils électromédicaux. Partie 2-47: Règles particulières de sécurité et performances essentielles des systèmes d'électrocardiographie ambulatoire.</i></p>
<b>CORRESPONDENCIA</b>	<p>Esta norma es la versión oficial, en español, de la Norma Europea EN 60601-2-47 de octubre de 2001, que a su vez adopta la Norma Internacional CEI 60601-2-47:2001.</p>
<b>OBSERVACIONES</b>	
<b>ANTECEDENTES</b>	<p>Esta norma ha sido elaborada por el comité técnico AEN/CTN 209 Equipos Electrónicos cuya Secretaría desempeña ANIEL.</p>

Edición e impresión por AENOR  
Depósito legal: M 34717-2002

© AENOR 2002  
Reproducción prohibida

LAS OBSERVACIONES A ESTE DOCUMENTO HAN DE DIRIGIRSE A:

**AENOR**

Asociación Española de  
Normalización y Certificación

C Génova, 6  
28004 MADRID-España

Teléfono: 91 432 60 00  
Fax: 91 310 40 32

46 Páginas

Grupo 28

AENOR AUTORIZA EL USO DE ESTE DOCUMENTO A SMART SOLUTIONS TECHNOLOGIES SL.  
Licencia para un usuario - Copia y uso en red prohibidos



American  
National  
Standard

ANSI/AAMI/  
IEC 60601-  
2-27:2011

Medical electrical  
equipment — Part 2-27:  
Particular requirements  
for the basic safety and  
essential performance  
of electrocardiographic  
monitoring equipment



Copyright Association for the Advancement of Medical Instrumentation. Provided by Document Center Inc. under license with AAMI. No reproduction or retransmission permitted without license from Document Center Inc.

Order: 083217 delivered by documentcenter.com on February 20, 2014





### 3. CD CONTENTS

- OrCAD Gerbers Folder
- LabView Project Folder
- Specifications Folder:
  - OP27
  - AMP02
  - PWR1726AC
  - MAX1044
  - ISO124
  - ESB33 CONMUTATOR
  - 1N1488 DIODE
  - NI USB-6001 DAQ DEVICE